

Supporting information

Rotaxanes as ^{19}F MRI agents: Threading for higher sensitivity

Lan Yang^{a,c,1}, Yu Li^{a,1}, Mou Jiang^{a,b,1}, Rui Zhou^{a,b}, Hengjiang Cong^c, Minghui Yang^{a,b}, Lei Zhang^{a,b}, Shenhui Li^{a,b}, Yunhuang Yang^{a,b}, Maili Liu^{a,b}, Xin Zhou^{a,b,d}, Zhong-Xing Jiang^{a,b,*}, Shizhen Chen^{a,b,d,*}

^aState Key Laboratory of Magnetic Resonance and Atomic and Molecular Physics, National Center for Magnetic Resonance in Wuhan, Wuhan Institute of Physics and Mathematics, Innovation Academy for Precision Measurement Science and Technology, Chinese Academy of Sciences-Wuhan National Laboratory for Optoelectronics, Wuhan 430071, China.

^bUniversity of Chinese Academy of Sciences, Beijing 100049, China.

^cSchool of Pharmaceutical Sciences & College of Chemistry and Molecular Sciences, Wuhan University, Wuhan 430071, China.

^dOptics Valley Laboratory, Wuhan 430074, China

Table of contents

1. General information.....	2
2. Synthesis and characterization of compounds.....	3
3. 2D ROESY ^1H NMR spectra of [2]rotaxanes Rx-2	10
4. ^{19}F diffusion coefficients (D) of macrocycle 1 , axle A₁ and [2]rotaxane Rx-1	10
5. T_1 and T_2 determination	11
6. ^{19}F MRI phantom experiments of macrocycle 1 , [2]rotaxanes Rx-2 and Rx-2'	13
7. Single-crystal X-ray data of macrocycle 1 and [2]rotaxane Rx-1	13
8. Molecular dynamics simulations	15
9. Solid-state NMR experiments	16
10. Copies of $^1\text{H}/^{13}\text{C}/^{19}\text{F}$ NMR and MS spectra of compounds.....	20

* Corresponding author.

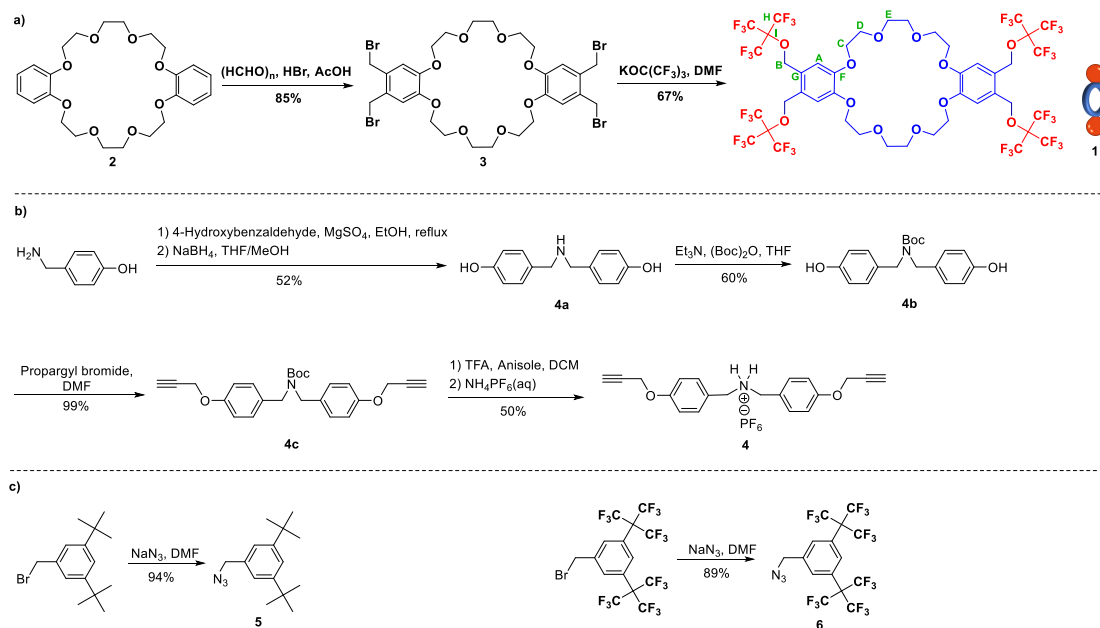
E-mail address: zxjiang@apm.ac.cn (Z.-X. Jiang), chenshizhen@apm.ac.cn (S. Chen).

¹These authors contributed equally to this work.

1. General information

^1H , ^{13}C and ^{19}F NMR spectra were recorded on a Bruker 400 MHz or 500 MHz spectrometer. Chemical shifts were presented in ppm and coupling constants (J) were in Hertz (Hz). ^1H NMR spectra were referenced to deuterated solvents, including CDCl_3 (s, 7.26 ppm), acetone- d_6 (s, 2.05 ppm), CD_3CN (s, 1.94 ppm). ^{13}C NMR spectra were referenced to solvent carbons (1.32 ppm for CD_3CN , 29.84 ppm for acetone- d_6). ^{19}F NMR spectra were referenced to 2% perfluorobenzene (s, -164.90 ppm) in CD_3CN . The splitting patterns for ^1H NMR spectra were denoted as follows: s (singlet), d (doublet), t (triplet), q (quartet), m (multiplet), b (broad), and combinations thereof. High-resolution mass spectra (HRMS) were recorded on a Thermo Fisher Scientific Q Exactive Focus. The single-crystal X-ray diffraction data for macrocycle **1** and [2]rotaxane **Rx-1** were collected using Rigaku XtaLAB PRO MM007HF and Rigaku XtaLAB P200. MALDI-ICR mass spectra were recorded on a 9.4 T SolariX FT-ICR-MS using the single MS mode for positive ions with dithranol as a matrix.

2. Synthesis and characterization of compounds



Scheme S1. The synthesis of macrocycle **1**, compound **4**, and stoppers **5** and **6**.

Crown ether 3 [1]: Dibenzo 24-crown-8 (0.50 g, 1.11 mmol), paraformaldehyde (0.30 g, 9.99 mmol), and hydrobromic acid (33% water solution) were suspended in acetic acid (8.00 mL), the reaction was stirred at 60 °C until all the solids were dissolved (about 1 day). The mixture was then left to stand without stirring for another 2 days to allow the precipitation of a white product. The solid was collected by filtration, washed consecutively with water, ethanol, and diethyl ether, and then air-dried. Crown ether **3** was obtained as a white solid (0.78 g, yield 85%), which was directly used in the next step without further purification. ¹H NMR (400 MHz, CDCl₃) δ 6.82 (s, 4H, H_A), 4.59 (s, 8H, H_B), 4.15 (s, 8H, H_C), 3.91 (s, 8H, H_D), 3.80 (s, 8H, H_E).

Macrocycle 1: Crown ether **3** (1.22 g, 1.49 mmol) and potassium perfluoro-*tert*-butoxide (2.45 g, 8.94 mmol) were dissolved in a mixed solvent of *N,N*-dimethyl formaldehyde/tetrahydrofuran (DMF/THF, 1/1, 20 mL), the reaction was stirred overnight at room temperature. After thin-layer chromatography (TLC) showed that the reaction was completed, water (150 mL) was added to the reaction mixture which was extracted with ethyl acetate (EtOAc, 60 mL × 3). The organic layers were collected, dried over anhydrous sodium sulfate, and evaporated under reduced pressure. The residue was purified by flash column chromatography on silica gel (petroleum ether (PE)/EtOAc = 2/1) to give macrocycle **1** as a white wax (1.43 g, yield 67%). ¹H NMR (500 MHz, CD₃CN) δ 7.01 (s, 4H, H_A), 5.11 (s, 8H, H_B), 4.13–4.15 (m, 8H,

H_C), 3.79-3.81 (m, 8H, H_D), 3.67 (s, 8H, H_E). ¹⁹F NMR (471 MHz, CD₃CN) δ -71.32 (s, F_A). ¹³C NMR (126 MHz, CD₃CN) δ 150.4 (C_F), 127.4 (C_G), 121.4 (q, *J* = 289.8 Hz, C_I), 116.5 (C_A), 80.4-81.1 (m, C_H), 71.7 (C_B), 70.4 (C_C), 70.04 (C_D), 70.01 (C_E). HRMS (ESI⁺) *m/z*: [M+Na]⁺ calculated for C₄₄H₃₆F₃₆NaO₁₂⁺ 1463.1524; found 1463.1524.

Compound 4a [2]: To a solution of 4-hydroxybenzaldehyde (4.89 g, 40.00 mmol) in anhydrous ethanol (120 mL) was added 4-hydroxybenzylamine (4.93 g, 40.00 mmol) and anhydrous magnesium sulfate (5.78 g, 48.00 mmol) under an argon atmosphere. The reaction was refluxed for 24 h, then the solvent was removed under reduced pressure and the residue was dissolved in a mixture of THF (60 mL) and MeOH (60 mL). NaBH₄ (6.05 g, 160.00 mmol) was slowly added in 10 portions at room temperature. The resulting mixture was stirred overnight and quenched with saturated ammonium chloride solution. THF and MeOH were removed under reduced pressure, the aqueous phase was extracted with ethyl ether (60 mL × 3). The combined organic layers were dried over anhydrous sodium sulfate. After removal of the solvent under reduced pressure, the residue was purified by flash column chromatography on silica gel (PE/EtOAc = 1/9) to give compound **4a** as a yellow wax (5.54 g, yield 60%). ¹H NMR (400 MHz, acetone-*d*₆) δ 7.17 (d, *J* = 8.6 Hz, 4H), 6.77 (d, *J* = 8.6 Hz, 4H), 3.64 (s, 4H).

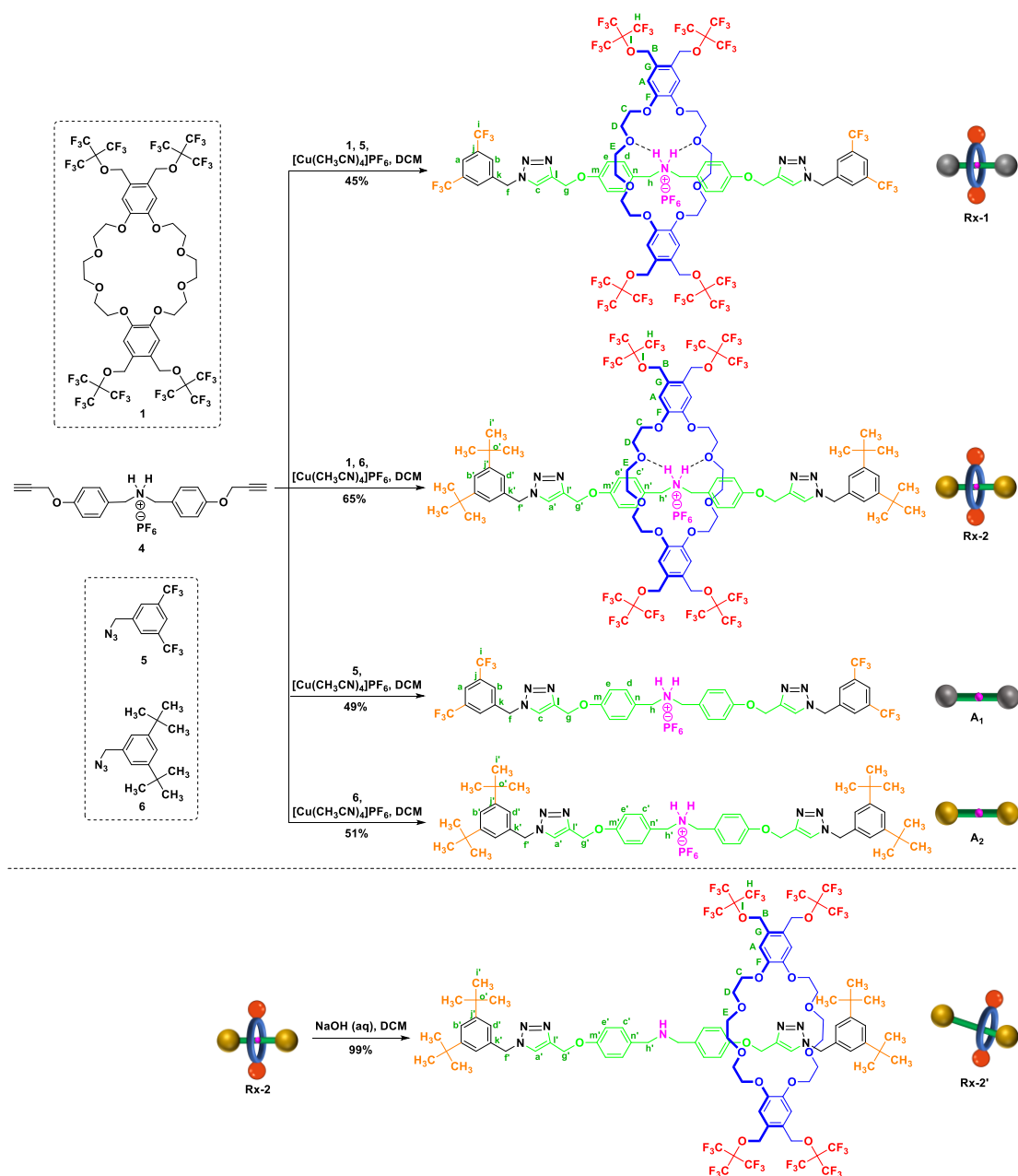
Compound 4b [3]: To a solution of compound **4a** (4.70 g, 20.50 mmol) in 100 mL of THF at 0 °C was added triethylamine (3.71 mL, 26.60 mmol) under an argon atmosphere, and the resulting mixture was stirred for 10 min. Then di-*tert*-butyl dicarbonate (6.71 g, 30.75 mmol) was slowly added to the mixture, the reaction was stirred overnight at room temperature. After removal of the solvent under reduced pressure, the residue was purified by flash column chromatography on silica gel (PE/EtOAc = 2/1) to give compound **4b** as a white solid (4.02 g, yield 60%). ¹H NMR (400 MHz, acetone-*d*₆) δ 8.38 (s, 2H), 7.10 (d, *J* = 7.3 Hz, 4H), 6.80-6.82 (m, 4H), 4.22-4.28 (m, 4H), 1.48 (s, 9H).

Compound 4c [4]: To a suspension of sodium hydride (1.20 g, 30.00 mmol, 60% in mineral oil) and compound **4b** (3.30 g, 10.00 mmol) in 50 mL of DMF was added 3-bromopropyne (2.74 mL, 35.00 mmol) at 0 °C. The resulting mixture was stirred at room temperature overnight. The reaction was quenched with 30 mL of saturated ammonium chloride solution and extracted with diethyl ether (30 mL × 3). The combined organic layers were washed with brine, dried over anhydrous sodium sulfate, and concentrated under reduced pressure. The residue was purified by flash column chromatography on silica gel (PE/EtOAc = 10/1) to give compound **4c** as a yellowish oil (4.03 g, yield 99%). ¹H NMR (400 MHz, CDCl₃) δ 7.13-7.16 (m, 4H), 6.93 (d, *J* = 8.7 Hz, 4H), 4.69 (d, *J* = 2.4 Hz, 4H), 4.25-4.33 (m, 4H), 2.53 (t, *J* = 2.4 Hz, 2H), 1.50 (s, 9H).

Compound 4 [5]: At room temperature, trifluoroacetic acid (9.55 mL, 129.00 mmol) and anisole (1.06 mL, 9.75 mmol) were added to a solution of compound **4c** (2.62 g, 6.46 mmol) in 50 mL of DCM, the resulting mixture was stirred for 12 h. The reaction mixture was concentrated under reduced pressure to give a residue as a white solid (2.68 g, yield 99%), which was directly used in the next step without further purification. To a solution of the residue (0.54 g, 1.28 mmol) in 9 mL of methanol was added 18 mL of a saturated aqueous solution of NH₄PF₆, and the resulting mixture was stirred for 5 h at room temperature. The reaction mixture was extracted with 100 mL of dichloromethane and the organic layer was collected. The organic layer was evaporated under reduced pressure to give the crude product, which was purified by flash column chromatography on silica gel (DCM/MeOH = 10/1) to afford compound **4** as a yellowish wax (0.56 g, yield 97%). ¹H NMR (400 MHz, CDCl₃) δ 7.27 (d, *J* = 8.6 Hz, 4H), 6.94 (d, *J* = 8.7 Hz, 4H), 4.68 (d, *J* = 2.4 Hz, 4H), 3.74 (s, 4H), 2.52 (t, *J* = 2.4 Hz, 2H). ¹³C NMR (101 MHz, acetone-*d*₆) δ 159.4, 132.6, 124.8, 116.0, 79.4, 77.3, 56.2, 51.8. HRMS (ESI⁺) *m/z*: [M-PF₆⁻]⁺ calculated for C₂₀H₂₀NO₂⁺, 306.1489; found, 306.1485.

Stopper 5 [6]: To a solution of 3,5-bis(trifluoromethyl)benzyl bromide (3.07 g, 10.00 mmol) in DMF (30 mL) was added sodium azide (0.98 g, 15.00 mmol) under an argon atmosphere, the reaction was stirred at 80 °C overnight. The reaction mixture was cooled to room temperature, diluted with water (60 mL), and extracted with EtOAc (80 mL × 3). The combined organic layers were washed with brine (100 mL × 3), dried with anhydrous sodium sulfate, and concentrated under reduced pressure to give stopper **5** as a yellowish oil (2.52 g, yield 94%). ¹H NMR (400 MHz, CDCl₃) δ 7.86 (s, 1H), 7.79 (s, 2H), 4.56 (s, 2H).

Stopper 6 [7]: Stopper **6** was prepared from 3,5-di-*tert*-butylbenzyl bromide (10.00 g, 35.30 mmol) by following the same procedure for the synthesis of stopper **6** as a clear oil (8.30 g, yield 96%). ¹H NMR (400 MHz, CDCl₃) δ 7.42 (t, *J* = 1.8 Hz, 1H), 7.16 (d, *J* = 1.8 Hz, 2H), 4.35 (s, 2H), 1.36 (s, 18H).



Scheme S2. The synthesis of macrocycle **1**, [2]rotaxanes **Rx-1**, **Rx-2**, and **Rx-2'**, and axles **A1** and **A2**.

[2]Rotaxane Rx-1: A mixture of compound **4** (40.00 mg, 0.089 mmol) and macrocycle **1** (255.30 mg, 0.18 mmol) was stirred for 0.5 h in dry dichloromethane under an argon atmosphere at room temperature. Then stopper **5** (71.50 mg, 0.27 mmol) and $[\text{Cu}(\text{CH}_3\text{CN})_4]\text{PF}_6$ (66.10 mg, 0.18 mmol) were added and the resulting mixture was stirred for an additional 2 days. The reaction was concentrated under vacuum and the residue was purified by flash column chromatography on silica gel (dichloromethane: methanol = 50 : 1) to give [2]rotaxane **Rx-1** as clear wax (97.70 mg, yield 45%). ^1H NMR (500 MHz, CD_3CN) δ

8.00 (s, 2H, H_a), 7.90 (s, 6H, H_{b,c}), 7.29 (d, $J = 8.6$ Hz, 4H, H_d), 6.86 (s, 4H, H_A), 6.74 (d, $J = 8.6$ Hz, 4H, H_c), 5.71 (s, 4H, H_f), 5.11 (s, 8H, H_B), 4.95 (s, 4H, H_g), 4.59-4.61 (m, 4H, H_h), 4.08 (d, $J = 2.5$ Hz, 8H, H_C), 3.79 (d, $J = 3.5$ Hz, 8H, H_D), 3.67 (s, 8H, H_E). ¹⁹F NMR (471 MHz, CD₃CN) δ -64.00 (s, 12F, F_B), -71.32 (s, 36F, F_A), -73.29 (d, $J = 706.5$ Hz, 6F, F_C). ¹³C NMR (126 MHz, CD₃CN) δ 159.8 (C_m), 148.9 (C_F), 144.6 (C_i), 139.7 (C_k), 132.6 (q, $J = 25.2$ Hz, C_j), 131.9 (C_n), 129.8 (C_c), 127.4 (C_G), 125.5 (C_d), 125.2 (C_b), 124.4 (q, $J = 277.2$ Hz, C_i), 123.4 (C_a), 121.4 (q, $J = 289.8$ Hz, C_l), 115.5 (C_A), 115.0 (C_e), 80.4-81.1 (m, C_H), 71.8 (C_E), 71.0 (C_D), 70.0 (C_C), 69.2 (C_B), 62.3 (C_g), 53.2 (C_f), 52.8 (C_h). MALDI-ICR-MS m/z : [M-PF₆]⁺ calculated for C₈₂H₆₆F₄₈N₇O₁₄⁺, 2284.3896; found, 2284.3880.

[2]Rotaxane Rx-2: [2]Rotaxane **Rx-2** was prepared from stopper **6** (65.20 mg, 0.27 mmol), compound **4** (40.00 mg, 0.089 mmol) and macrocycle **1** (255.30 mg, 0.18 mmol) by following the same procedure for the synthesis of [2]rotaxane **Rx-1** as a clear wax (136.70 mg, yield 65%). ¹H NMR (500 MHz, CD₃CN) δ 7.81 (s, 2H, H_{a'}), 7.44 (t, $J = 1.8$ Hz, 2H, H_{b'}), 7.27 (d, $J = 8.7$ Hz, 4H, H_{c'}), 7.20 (d, $J = 1.8$ Hz, 4H, H_{d'}), 6.87 (s, 4H, H_A), 6.74 (d, $J = 8.7$ Hz, 4H, H_{c'}), 5.50 (s, 4H, H_F), 5.14 (s, 8H, H_B), 4.93 (s, 4H, H_{g'}), 4.57-4.60 (m, 4H, H_{h'}), 4.08-4.09 (m, 8H, H_C), 3.77-3.78 (m, 8H, H_D), 3.65 (s, 8H, H_E), 1.27 (s, 36H, H_{i'}). ¹⁹F NMR (471 MHz, CD₃CN) δ -71.27 (s, 36F, F_A), -73.36 (d, $J = 706.5$ Hz, 6F, F_C). ¹³C NMR (126 MHz, CD₃CN) δ 159.8 (C_{m'}), 152.6 (C_{j'}), 148.9 (C_F), 144.2 (C_{i'}), 136.0 (C_{n'}), 131.9 (C_{k'}), 127.5 (C_G), 125.4 (C_{e'}), 124.6 (C_{d'}), 123.5 (C_{a'}), 123.5 (C_{b'}), 121.4 (q, $J = 289.8$ Hz, C_l), 115.6 (C_A), 115.0 (C_{e'}), 80.4-81.1 (m, C_H), 71.8 (C_E), 71.0 (C_D), 70.0 (C_C), 69.2 (C_B), 62.2 (C_{g'}), 55.0 (C_F), 52.8 (C_{h'}), 35.5 (C_{o'}), 31.5 (C_{i'}). MALDI-ICR-MS m/z : [M-PF₆]⁺ calculated for C₉₄H₁₀₂F₃₆N₇O₁₄⁺, 2236.6904; found, 2236.6874.

[2]Rotaxane Rx-2': [2]Rotaxane **Rx-2** (50 mg, 0.02 mmol) was dissolved in 100 mL of dichloromethane and washed with NaOH solution (1 mol/L, 100 mL \times 3). The resulting solution was dried with anhydrous magnesium sulfate and concentrated under vacuum to give [2]rotaxane **Rx-2'** (46.50 mg, yield 99%). ¹H

NMR (500 MHz, CD₃CN) δ 8.14 (s, 2H, H_a'), 7.41 (s, 2H, H_b'), 7.18 (d, J = 1.6 Hz, 4H, H_d'), 7.07 (d, J = 7.9 Hz, 4H, H_c'), 6.98 (s, 4H, H_A), 6.93 (d, J = 7.9 Hz, 4H, H_e'), 5.41 (s, 4H, H_F'), 5.33 (s, 4H, H_G'), 5.12 (s, 8H, H_B), 4.05-4.06 (m, 8H, H_C), 3.61 (s, 8H, H_D), 3.56 (s, 4H, H_h'), 3.16 (s, 8H, H_E), 1.27 (s, 18H, H_{ia}'), 1.24 (s, 18H, H_{ib}'). ¹⁹F NMR (471 MHz, CD₃CN) δ -71.27 (s, 36F, F_A). ¹³C NMR (126 MHz, CD₃CN) δ 158.6 (C_m'), 152.5 (C_j'), 150.0 (C_F'), 145.8 (C_I'), 136.2 (C_n'), 129.8 (C_k'), 127.0 (C_G'), 125.3 (C_e'), 124.6 (C_d'), 123.6 (C_a'), 123.5 (C_b'), 121.4 (q, J = 293.0 Hz, C_I), 115.7 (C_A), 115.0 (C_e'), 80.4-81.1 (m, C_H), 71.7 (C_E), 70.4 (C_D), 70.05 (C_C), 69.5 (C_B), 62.8 (C_g'), 54.9 (C_F'), 53.0 (C_h'), 35.5 (C_o'), 31.6 (C_i'). MALDI-ICR-MS m/z : [M+H]⁺ calculated for C₉₄H₁₀₂F₃₆N₇O₁₄⁺, 2236.6904; found, 2236.6902.

Axle A₁: To a solution of compound **4** (150.0 mg, 0.33 mmol) in DCM (6 mL) was added stopper **5** (244.6 mg, 1.00 mmol) and [Cu(CH₃CN)₄]PF₆ (247.7 mg, 0.66 mmol), which was stirred under an atmosphere of argon for 2 days at room temperature. The reaction mixture was diluted with 100 mL of dichloromethane, washed with ethylenediaminetetraacetic acid disodium solution (3 × 50 mL), dried over anhydrous magnesium sulfate, and concentrated under reduced pressure. The residue was purified by flash column chromatography on silica gel (DCM/MeOH = 30/1) to give axle **A₁** as a yellowish wax (160.8 mg, yield 51%). ¹H NMR (500 MHz, CD₃CN) δ 7.87 (s, 2H, H_a'), 7.44 (s, 2H, H_b'), 7.29 (d, J = 8.4 Hz, 4H, H_c'), 7.20 (d, J = 1.3 Hz, 4H, H_d'), 6.98 (d, J = 8.4 Hz, 4H, H_e'), 5.50 (s, 4H, H_F'), 5.14 (s, 4H, H_G'), 3.90 (s, 4H, H_h'), 1.27 (s, 36H, H_i'). ¹³C NMR (126 MHz, CD₃CN) δ 159.4, 152.6, 144.6, 136.1, 131.7, 128.5, 124.7, 123.5, 123.5, 115.8, 62.4, 55.0, 52.2, 35.5, 31.6. HRMS (ESI⁺) m/z : [M-PF₆]⁺ calculated for C₅₀H₆₆N₇O₂⁺, 796.5273; found, 796.5270.

Axle A₂: Axle **A₂** was prepared from compound **4** (150.00 mg, 0.33 mmol), stopper **6** (244.60 mg, 1.00 mmol), and [Cu(CH₃CN)₄]PF₆ (247.70 mg, 0.66 mmol) by following the same procedure for the synthesis of Axle **A₁** as yellowish wax (160.80 mg, yield 51%). ¹H NMR (500 MHz, CD₃CN) δ 7.87 (s, 2H, H_a'), 7.44 (s, 2H, H_b'), 7.29 (d, J = 8.4 Hz, 4H, H_c'), 7.20 (d, J = 1.3 Hz, 4H, H_d'), 6.98 (d, J = 8.4 Hz, 4H, H_e'), 5.50 (s, 4H, H_F'), 5.14 (s, 4H, H_G'), 3.90 (s, 4H, H_h'), 1.27 (s, 36H, H_i'). ¹³C NMR (126 MHz, CD₃CN) δ 159.4 (C_m'), 152.6 (C_j'), 144.6 (C_I'), 136.1 (C_n'), 131.7 (C_k'), 128.5 (C_e'), 124.7 (C_d'), 123.5 (C_a'), 123.5

(C_b'), 115.8 (C_e'), 62.4 (C_g'), 55.0 (C_f'), 52.25 (C_h'), 35.5 (C_o'), 31.6 (C_i'). HRMS (ESI⁺) *m/z*: [M-PF₆]⁺

calculated for C₅₀H₆₆N₇O₂⁺, 796.5273; found, 796.5270.

3. 2D ROESY ¹H NMR spectra of [2]rotaxanes Rx-2

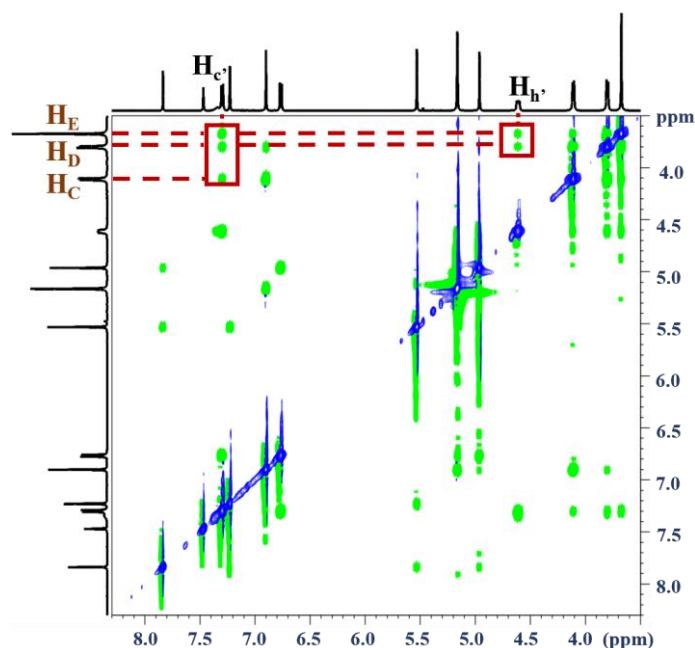


Fig. S1 2D ROESY ¹H NMR spectra of [2]rotaxanes **Rx-2**. NMR Conditions: 500 MHz, 1 mmol/L, 298 K, CD₃CN.

4. ¹⁹F diffusion coefficients (*D*) of macrocycle **1**, axle **A₁** and [2]rotaxane **Rx-1**

Measurements were performed on a Bruker 500 MHz spectrometer with CD₃CN as solvent at a concentration of 1.0 mM and 298 K. The sequence of ¹⁹F diffusion coefficients (*D*) was ledbpgp2s. DS = 4 and NS = 16.

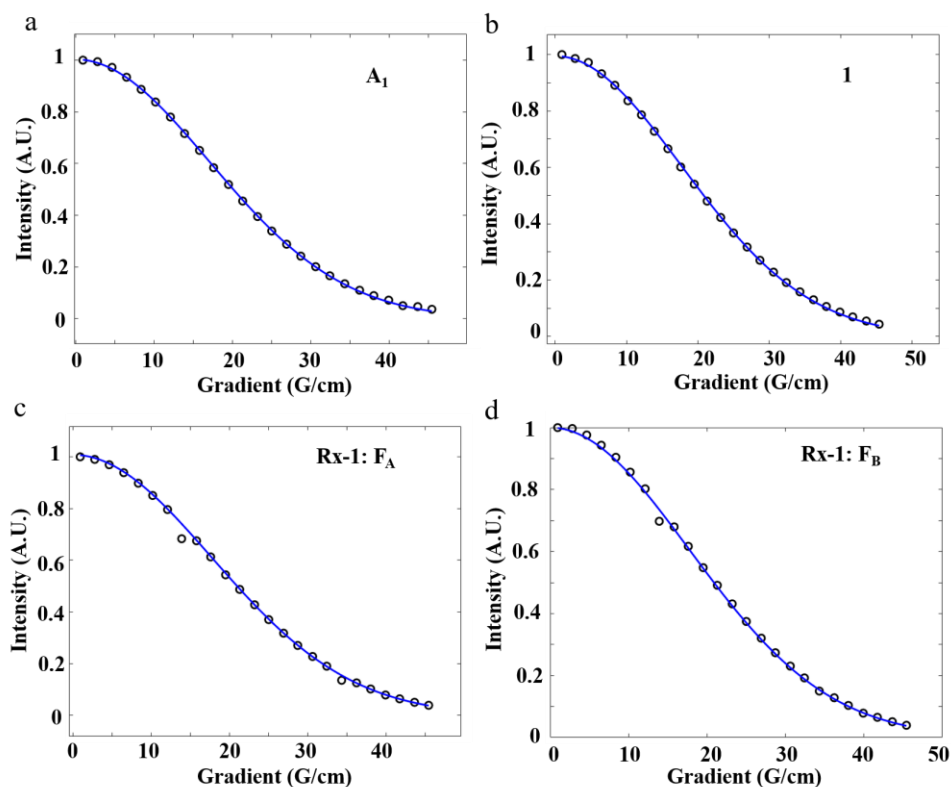


Fig. S2. 2D-DOSY fitting curve of axle A_1 , macrocycle **1**, and [2]rotaxane **Rx-1**.

Table S1: Diffusion coefficients (D) of ^{19}F in different compounds.

^{19}F NMR peaks	Compounds	Diffusion coefficients (D)
-71 ppm (F_A)	Macrocycle 1	$1.170 \times 10^{-9} \text{ m}^2/\text{s}$
	[2]Rotaxane Rx-1	$8.753 \times 10^{-10} \text{ m}^2/\text{s}$
-63 ppm (F_B)	Axle A_1	$1.135 \times 10^{-9} \text{ m}^2/\text{s}$
	[2]Rotaxane Rx-1	$8.742 \times 10^{-10} \text{ m}^2/\text{s}$

5. T_1 and T_2 determination

The pulse sequence for measuring T_1 was t1ir, T_1 values were extracted from a series of GRE images with recovery times 0.08, 0.2, 0.4, 0.8, 1.2, 1.6, 2.0, 2.6, 3.4, 4.2, 5.0, 6.0, 7.0, 9.0, 11.0, 15.0 s, and 16 averages. The pulse sequence for measuring T_2 was cpmg, T_2 values were extracted from a series of GRE images with recovery times 2000, 2200, 2400, 2800, 3200, 4000, 4800, 6000, 7200, 8600, 9400, 11000, 16000, 25000, 40000, 60000 s, and 16 averages.

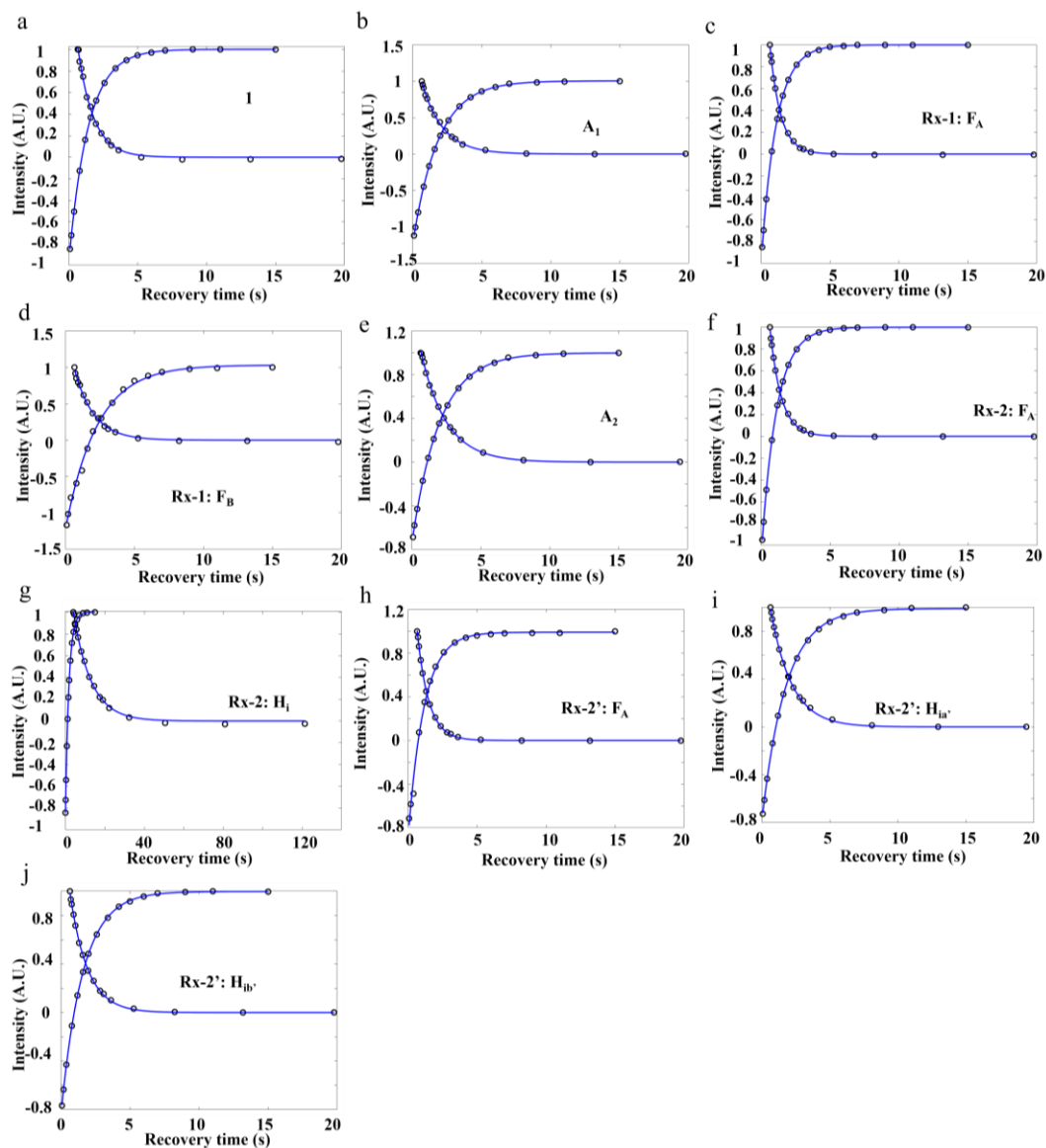


Fig. S3. Signal intensity (A.U.) vs recovery time (ms) collected for macrocycle **1**, axles **A₁** and **A₂**, and [2]rotaxanes **Rx-1**, **Rx-2**, and **Rx-2'**.

Table S2. T_1 and T_2 of F_A in the macrocycle, and [2]rotaxanes.

Compounds	1 (F_A)	Rx-1 (F_A)	Rx-2 (F_A)	Rx-2' (F_A)
T_1 (s)	1.406	1.079	1.103	1.112
T_2 (s)	1.052	0.750	0.763	0.762

Table S3. T_1 and T_2 of F_B and H_i in the axles, macrocycle, and [2]rotaxanes.

Compounds	A₁ (F_B)	Rx-1 (F_B)	A₂ (H)	Rx-2 (H)
T_1 (s)	1.827	1.692	2.001	1.771
T_2 (s)	1.409	1.296	1.666	1.496

6. ^{19}F MRI phantom experiments of macrocycle 1, [2]rotaxanes Rx-2 and Rx-2'

^{19}F MRI phantom experiments were performed on a Bruker BioSpec 400 MHz MRI system. The temperature of the magnet room was maintained at 24 °C during the experiment. The ^{19}F phantom images were acquired using a RARE pulse sequence, RARE factor = 4, matrix size = 32×32 , slice thickness = 20 mm, FOV = 3.0 cm \times 3.0 cm, TR = 600 ms, TE = 17.5 ms, scan time = 307 s.

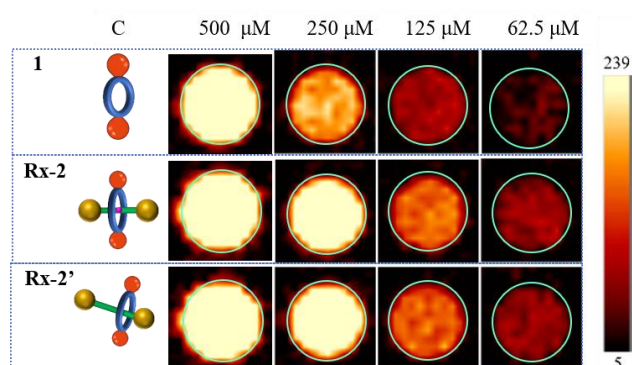


Fig. S4 ^{19}F MRI phantom images (9.4 T, 298 K, CH_3CN , concentration as indicated)

7. Single-crystal X-ray data of macrocycle 1 and [2]rotaxane Rx-1

Macrocycle 1: The crystal was grown from liquid-liquid diffusion in acetone and n-hexane (1 : 3) at 4 °C and acquired using $\text{CuK}\alpha$ ($\lambda = 1.54184 \text{ \AA}$) radiation. The crystal structure is deposited in the Cambridge Crystallographic Data Centre (CCDC Code: 2126397).

Crystal Data for $\text{C}_{50}\text{H}_{48}\text{F}_{36}\text{O}_{14}$ ($M = 1556.88 \text{ g/mol}$): Crystal size = $0.28 \times 0.22 \times 0.18 \text{ mm}^3$, Bond precision: C-C = 0.0050 \AA , Wavelength = 1.54184 \AA , $a = 23.1352(2) \text{ \AA}$, $b = 7.0743(1) \text{ \AA}$, $c = 18.6292(1) \text{ \AA}$, $\alpha = 90^\circ$, $\beta = 90.083(10)^\circ$, $\gamma = 90^\circ$, Temperature = 100 K, Volume = $3048.95(5) \text{ \AA}^3$, Space group P 1 21/c 1, Hall group -P 2ybc, Moiety formula $\text{C}_{44}\text{H}_{36}\text{F}_{36}\text{O}_{12}$, $2(\text{C}_3\text{H}_6\text{O})$ Sum formula $\text{C}_{50}\text{H}_{48}\text{F}_{36}\text{O}_{14}$, $M_r = 1556.88 \text{ g/mol}$, $D_{\text{calc}} = 1.696 \text{ g/cm}^3$, $Z = 4$, $\mu(\text{MuKa}) = 1.752 \text{ mm}^{-1}$, $F_{000} = 1568.0$, $(h, k, l_{\text{max}}) = (25, 7, 20)$, $N_{\text{ref}} = 4502$, $T_{\text{min}} = 0.582$, $T_{\text{max}} = 1.000$, Data completeness = 0.998, $\Theta(\text{max}) = 59.997$,

R(reflections) = 0.0549(4445), wR₂(reflections) = 0.1612(4502), S = 1.067, Npar = 466.

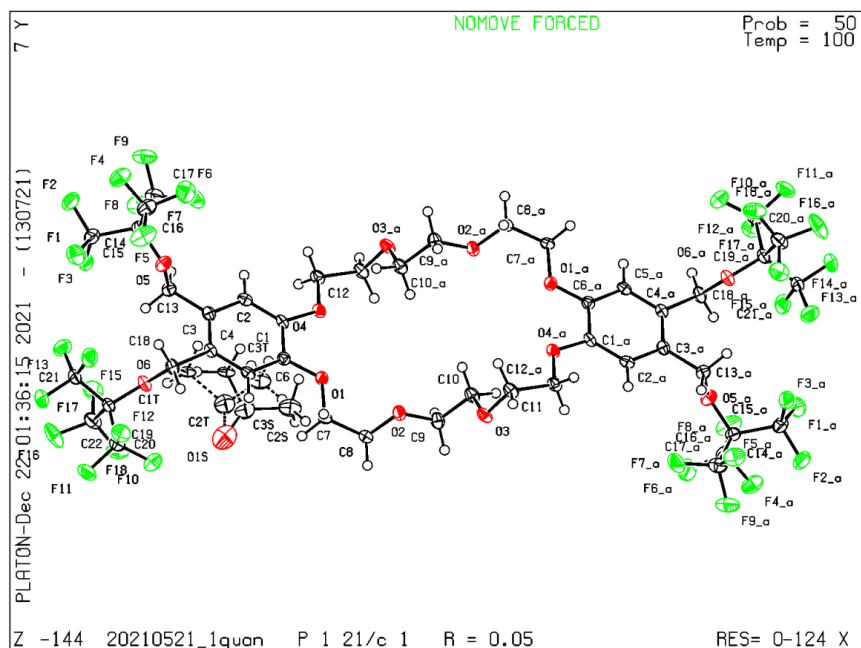


Fig. S5. X-Ray structure of **1** (50% probability level shown)

[2]Rotaxane Rx-1: The crystal was grown from liquid-liquid diffusion in ethyl ether and 2-butanone and n-hexane (0.5 : 0.5 : 3) at 15 °C and acquired using CuK α (λ = 1.54184 Å) radiation. The crystal structure is deposited in the Cambridge Crystallographic Data Centre (CCDC Code: 2126385).

Crystal Data for C₈₆H₇₄F₅₄N₇O₁₅P (M = 2502.49 g/mol): Crystal size = 0.04 × 0.04 × 0.02 mm³, Bond precision: C-C = 0.0079 Å, Wavelength = 1.54184 Å, a = 22.7294(2) Å, b = 19.3316(2) Å, c = 24.9762(3) Å, α = 90°, β = 95.655(10)°, γ = 90°, Temperature = 100 K, Volume = 10921.0(2) Å³, Space group P 1 21/c 1, Hall group -P 2ybc, Moiety formula F₆P, C₄₄H₃₆F₃₆O₁₂, C₃₈H₃₀F₁₂N₇O₂, C₄H₈O. Sum formula C₈₆H₇₄F₅₄N₇O₁₅P, Mr = 2502.49 g/mol, D_{calc} = 1.522 g/cm³, Z = 4, μ (MuKa) = 1.623 mm⁻¹, F₀₀₀ = 5040.0, (h, k, l_{max}) = (27, 23, 28), N_{ref} = 20174, T_{min} = 0.841, T_{max} = 1.000, Data completeness = 0.978, Theta(max) = 69.767, R(reflections) = 0.1479(15065), wR₂(reflections) = 0.4528(20174), S = 1.939, Npar = 1398.

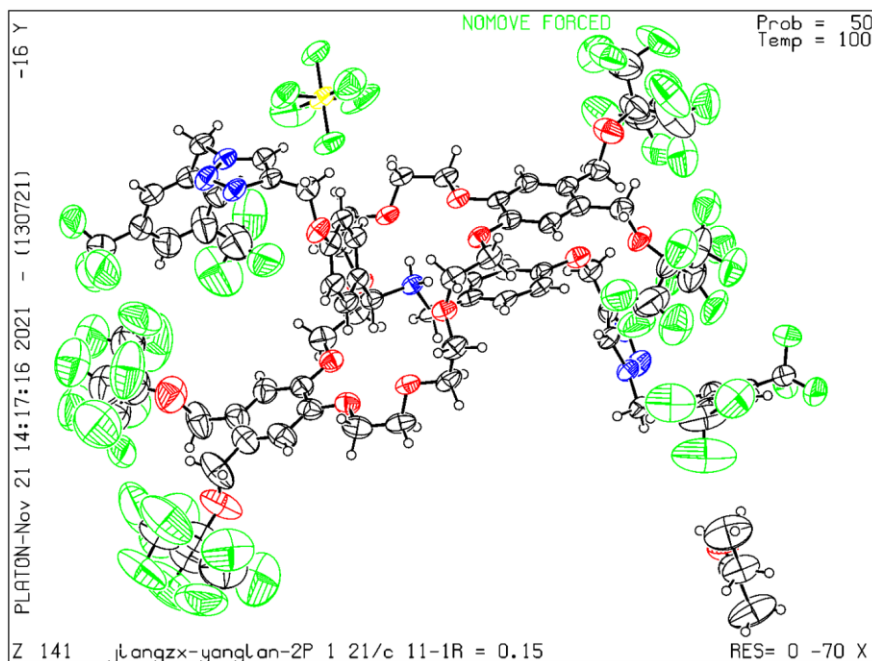


Fig. S6. X-Ray structure of **Rx-1** (50% probability level shown).

8. Molecular dynamics simulations

Based on the X-ray structure of pinwheel rotaxane, three modeling systems were constructed: the conformation of the rotaxane with pinwheels and axis; the pinwheels and axis conformation with the neutral charge at the center nitrogen atom; and the only pinwheels conformation. To obtain the initial configurations for the molecular dynamics (MD) simulations, each modeling system was packed at the center of the cube by the edges of 70Å, surrounded with 5000 individual solvent molecules of acetonitrile using the Packmol program [8].

All MD simulations were performed by the AMBER14 software package supported GPU computation with the CUDA version of the pmemd program [9]. The topology parameters of the modeling systems were generated by quantum mechanical HF/6-31G* optimizations from Gaussian09 software [10] cooperated with RESP [11] approach and GAFF [12] force field from AMBER package.

The conventional procedures were carried out to produce MD trajectories of each system. Firstly,

the systems of energy were minimized to relieve energetic strain from the packing procedure. Secondly, equilibration processes were conducted with the systems heated in constant volume (NVT ensemble) and equilibrated in constant pressure (NPT ensemble) conditions. During the heating process, the temperature was increased gradually from 0 K to 300 K by 10,000 steps with a time step of 2.0 fs, and then a further 10,000 steps were performed under the temperature of 300 K. During the subsequent process, the systems were equilibrated under the constant pressure of 1.0 bar using Berendsen barostat by 5 million steps in a 1.0 fs time step for 5 ns in total. Finally, the production MD simulations were performed for 30 ns under the identical procedure of equilibration in the NPT ensemble. Analyses of the trajectories were applied CPPTRAJ program [13] and in-house scripts.

To evaluate the ^{19}F -atom movements quantitatively, we calculated the distance root-mean-square deviation (Drmsd) [14] of ^{19}F atoms to the reference structure, the X-ray structure for the structural analysis. The definition of the Drmsd is expressed as:

$$Drmsd = \sqrt{\frac{1}{N_{pair}} \sum_{i=1}^N \sum_{j=i+1}^N (D_{ij} - D_{ref,ij})^2}$$

with $N_{pair} = \frac{1}{2} N(N - 1)$, where N denotes the total number of ^{19}F atoms of each conformation referring to the simulated and reference structures. D_{ij} is the distance between instantaneous positions of ^{19}F atoms of each frame along the simulated trajectories, and $D_{ref,ij}$ represents the corresponding distance of the ^{19}F -atom pairs in the reference structure. The Drmsd values provide the similarity measures of the inter ^{19}F -atom positions to the reference structure.

9. Solid-state NMR experiments

The rotational motions were quantified using “rotational correlation time (τ_c)”. We carried out ^{19}F magic angle (MAS) NMR experiments, a well-established tool for probing τ_c [15-17], on macrocycle **1**

and [2]rotaxane **Rx-2** in solid state (Figure S7a-S7d). The ^{19}F relaxation rates R_1 and R_2 are composed of the heteronuclear dipole interaction (q_{DD}) and the chemical shift anisotropy (q_{CSA}) of the ^{19}F atom, which can be obtained from the following Equations [15]:

$$R_1 = \sum q_{DD} [J(\omega_F - \omega_H) + 3J(\omega_F) + 6J(\omega_F + \omega_H)] + q_{CSA}J(\omega_F) \quad [1]$$

$$R_2 = \frac{1}{2} \sum q_{DD} [4J(0) + J(\omega_F - \omega_H) + 3J(\omega_F) + 6J(\omega_H) + 6J(\omega_F + \omega_H)] + \frac{1}{6} q_{CSA} [4J(0) + 3J(\omega_F)] \quad [2]$$

$$q_{CSA} = \frac{2}{15} \omega_F^2 \left(1 + \frac{\eta_{CSA}^2}{3} \right) \Delta\delta^2 \quad [3]$$

$$q_{DD} = \frac{1}{10} \left(\frac{\mu_0}{4\pi} \right) \hbar^2 \gamma_F^2 \gamma_H^2 r_{HF}^{-6} \quad [4]$$

$$J(\omega) = \frac{\tau_c}{1 + (\omega\tau_c)^2} \quad [5]$$

Where δ_σ is the chemical shift anisotropy of the ^{19}F atom ($\delta_\sigma = \delta_{33} - (\delta_{11} + \delta_{22} + \delta_{33})/3$) measured by solid-state NMR, and the three different δ represent the chemical shift tensor in three different directions, respectively. The asymmetry parameter η_{CSA} was given by $\eta_{CSA} = (\delta_{22} - \delta_{11})/\delta_\sigma$. γ_H and γ_F represent the gyromagnetic ratio of ^1H and ^{19}F , while ω_H and ω_F denote the Larmor frequency of ^1H and ^{19}F , respectively. The other parameters are vacuum permeability (μ_0), reduced Planck constant (\hbar), and inter-nuclear distance (r_{HF}) between ^1H and ^{19}F .

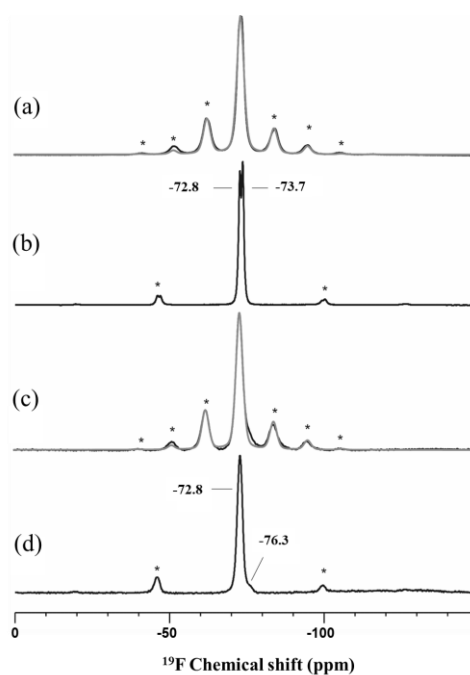


Fig. S7. ^{19}F DP-MAS NMR spectra of macrocycle **1** (a, b) and [2]rotaxane **Rx-2** (c, d) collected at the

spinning rates of 4 kHz (a, c) and 10 kHz (b, d).

Combined with the measured relaxation rates (R_I and R_2), we obtained the rotational correlation times (τ_c) for macrocycle **1** and [2]rotaxane **Rx-2**, as shown in Figure S8.

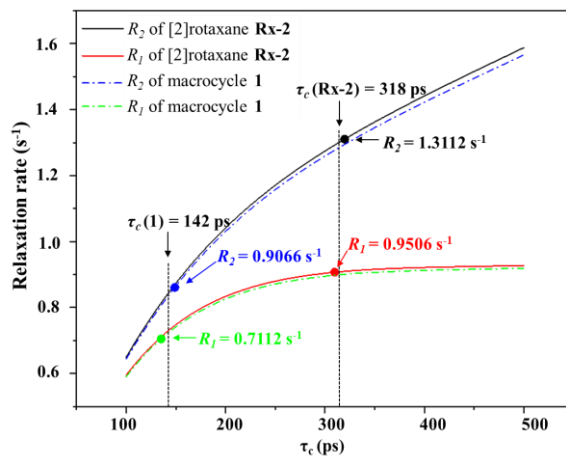


Fig. S8. The plot of relaxation rate and rotational correlation time of macrocycle **1** and [2]rotaxane **Rx-2**.

Table S4. ^{19}F CSA parameters (in ppm) of CF_3 groups in macrocycle **1** and [2]rotaxanes extracted from the DMFIT software package.

sample	δ_{11}	δ_{22}	δ_{33}	δ_σ
Macrocycle 1	-59.96	-68.94	-90.85	-17.60
[2]rotaxane Rx-2	-58.95	-68.34	-91.83	-18.79

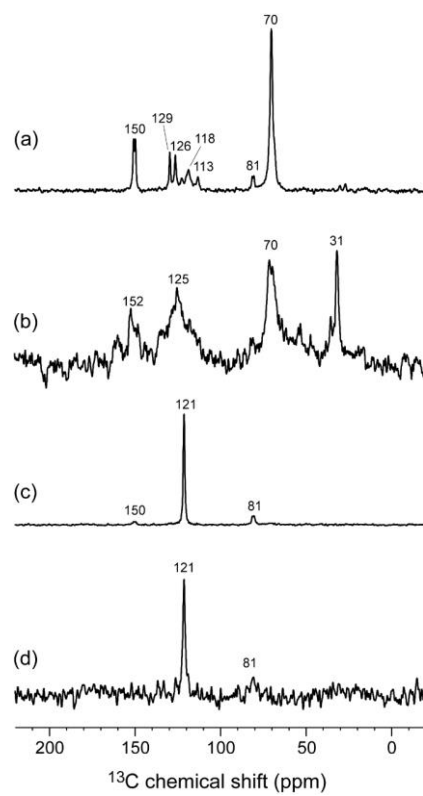
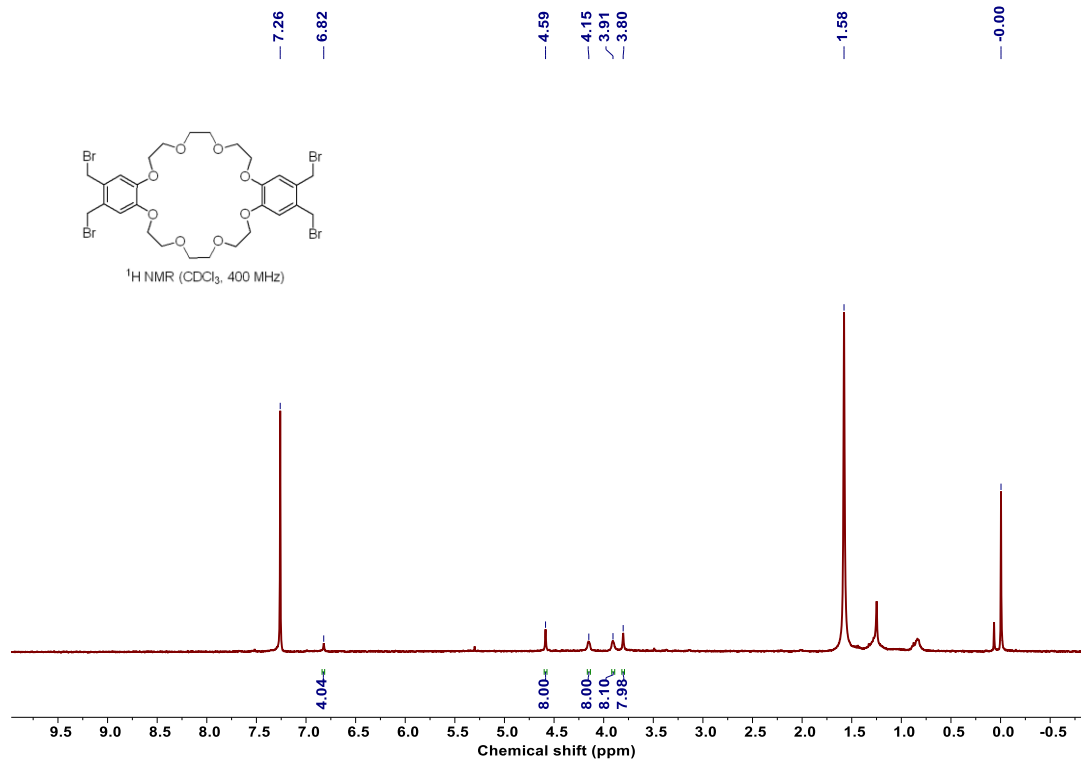


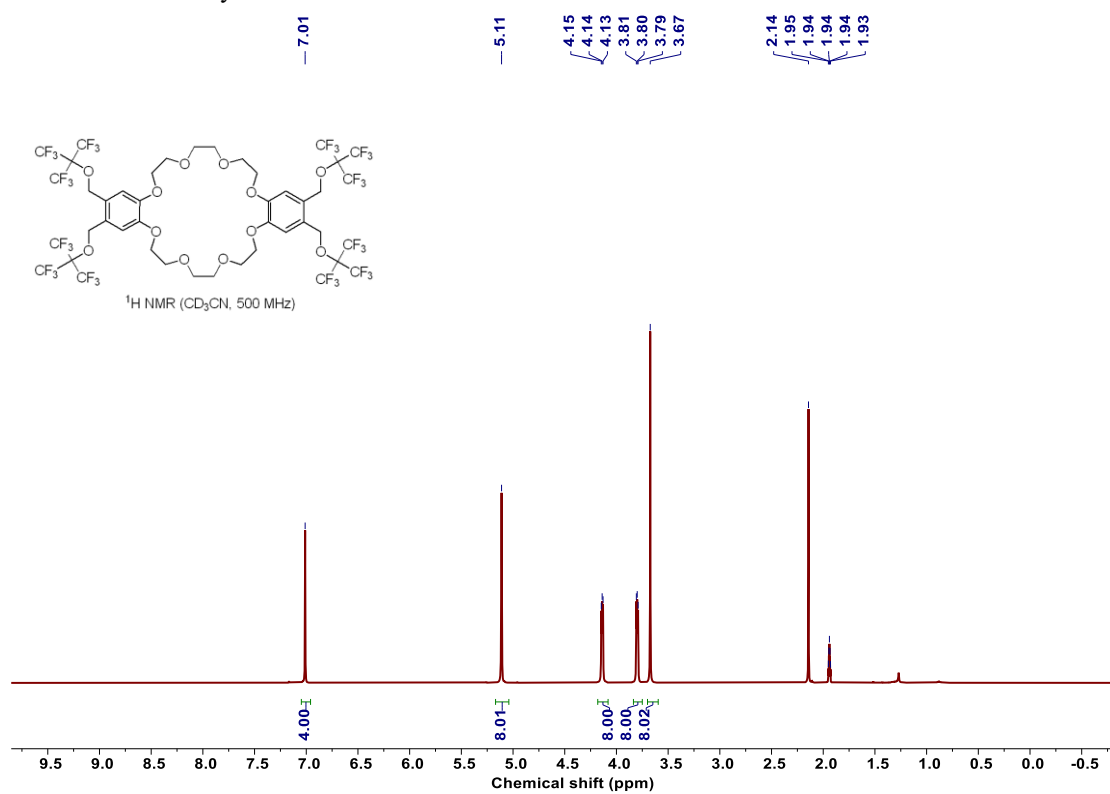
Fig. S9. $^1\text{H} \rightarrow ^{13}\text{C}$ (a, b) and $^{19}\text{F} \rightarrow ^{13}\text{C}$ (c, d) CP/MAS NMR spectra of macrocycle **1** and [2]rotaxane **Rx-2**. a, c belongs to macrocycle **1**, and b, d belongs to [2]rotaxane **Rx-2**.

10. Copies of $^1\text{H}/^{13}\text{C}/^{19}\text{F}$ NMR and MS spectra of compounds

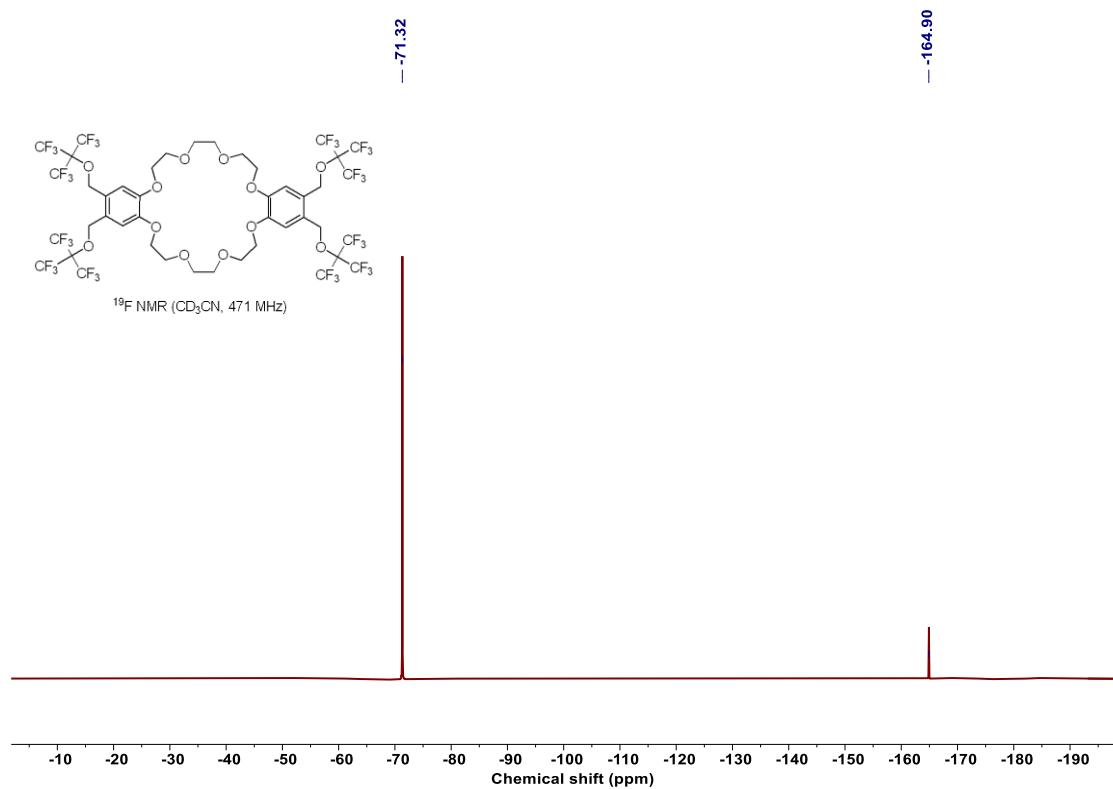
^1H NMR of crown ether **3**



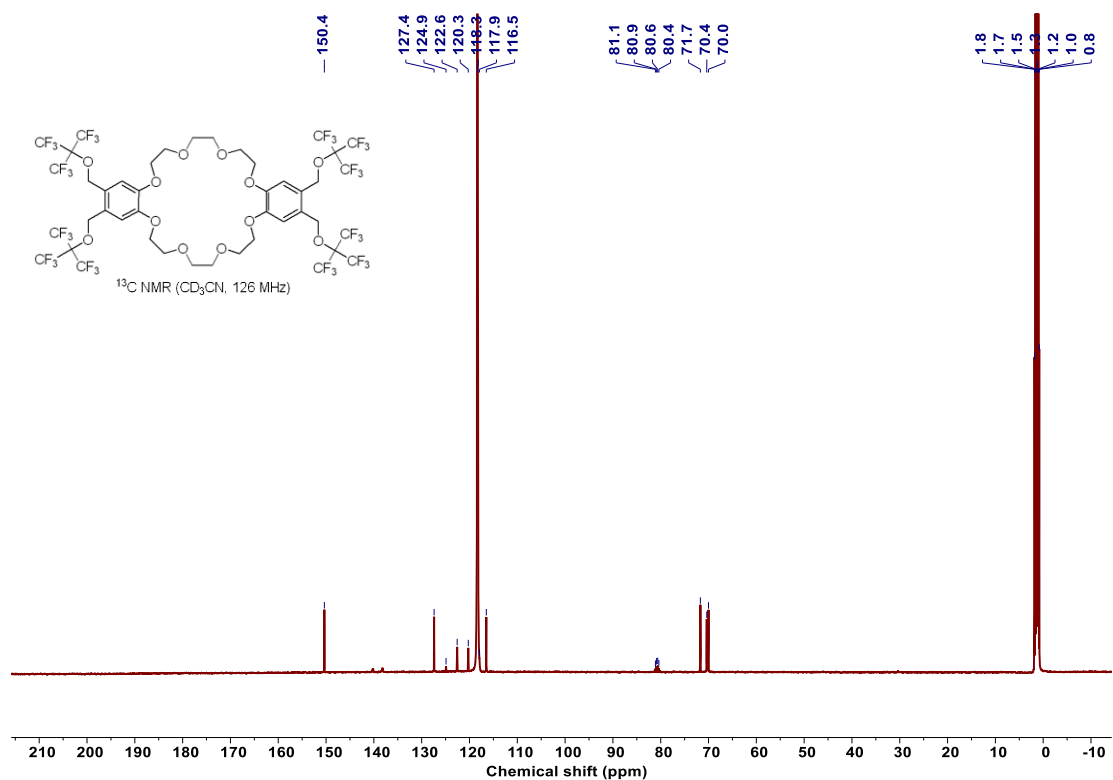
^1H NMR of macrocycle **1**



^{19}F NMR of macrocycle **1**

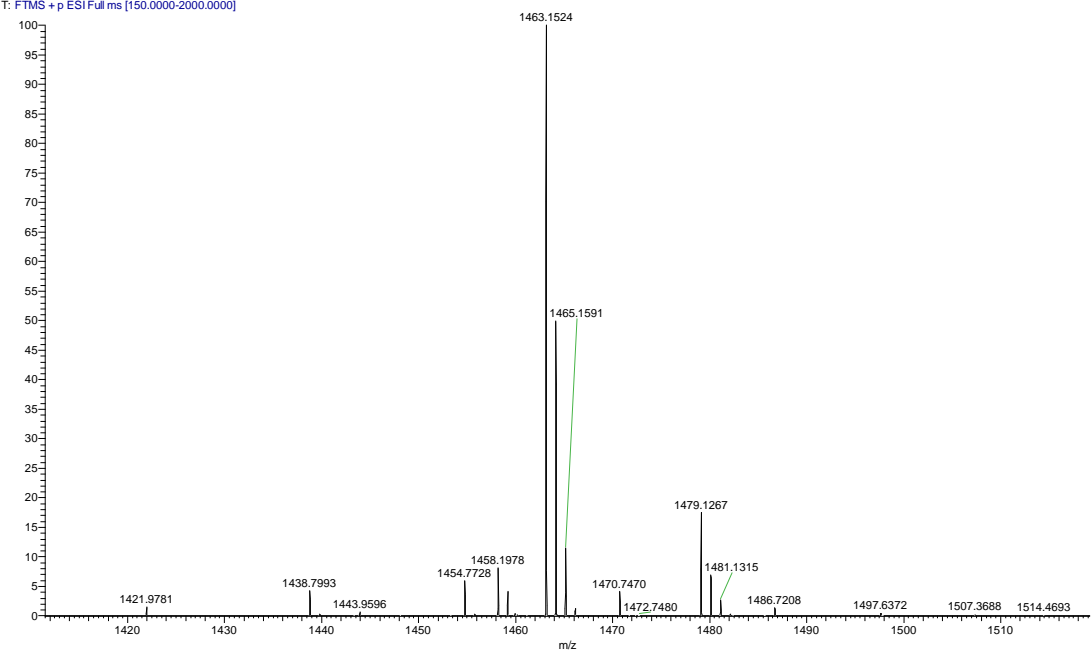


^{13}C NMR of macrocycle **1**

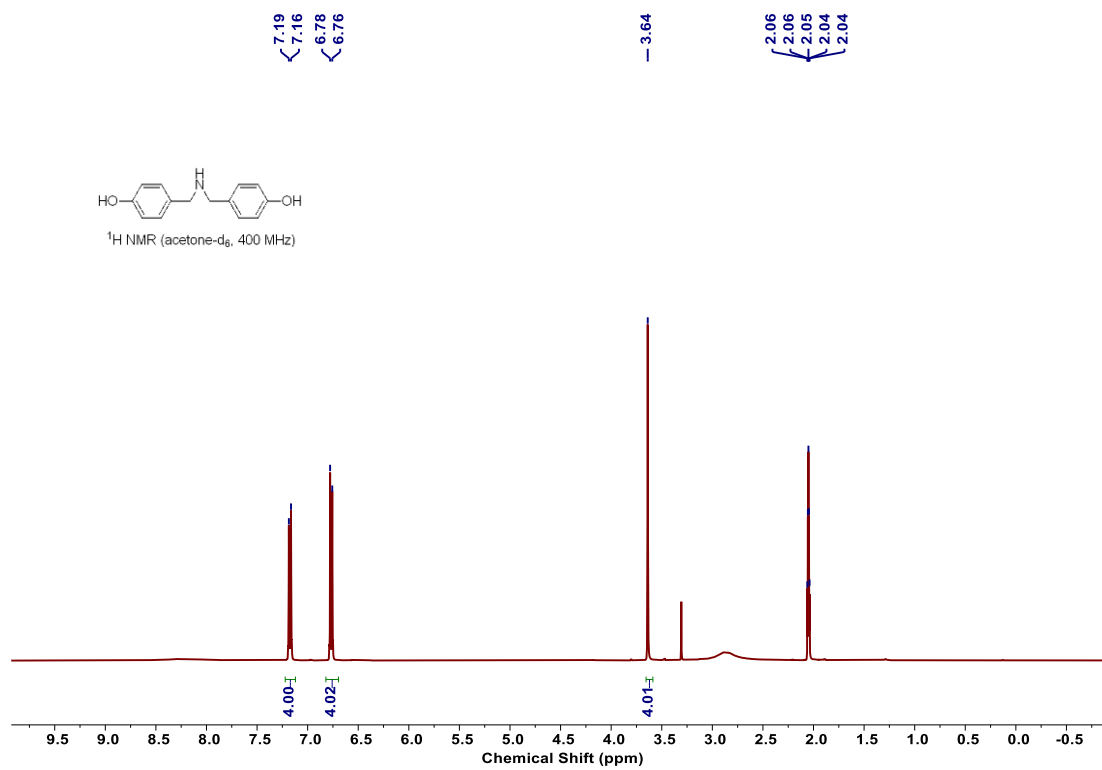


HRMS of macrocycle 1

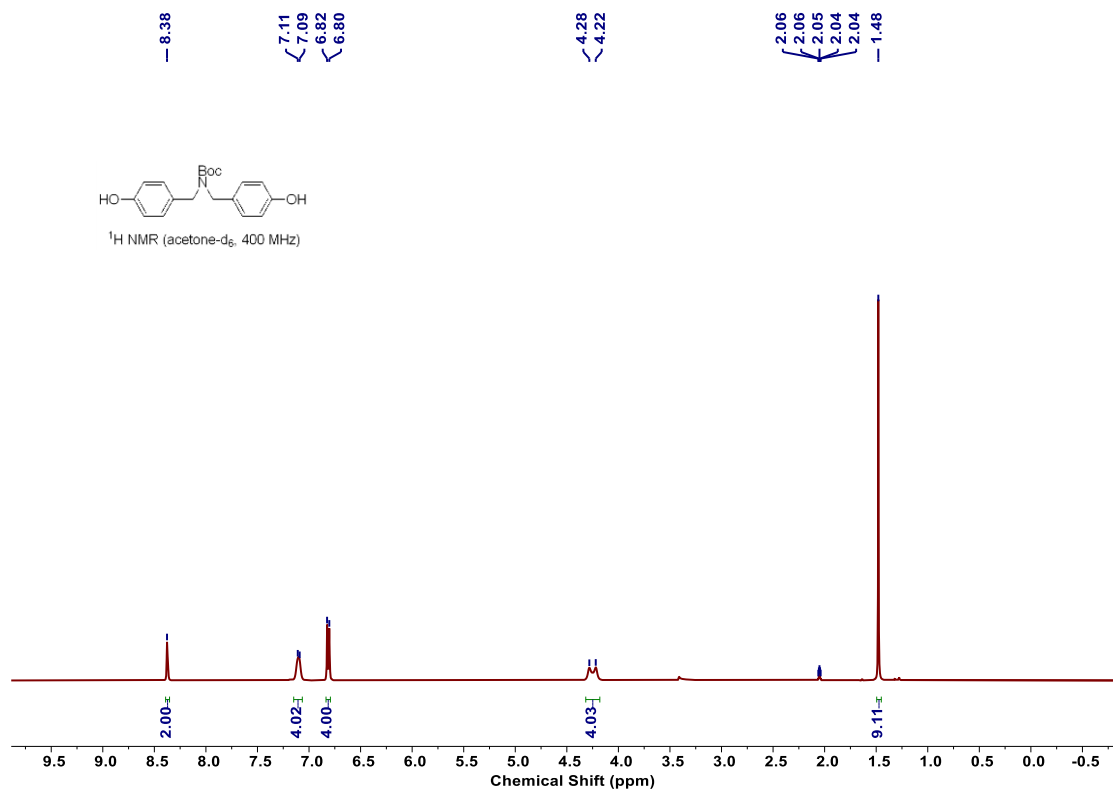
1 #1200-1243 RT: 11.73-12.14 AV: 22 NL: 1.19E6
T: FTMS + p ESI Full ms [150.0000-2000.0000]



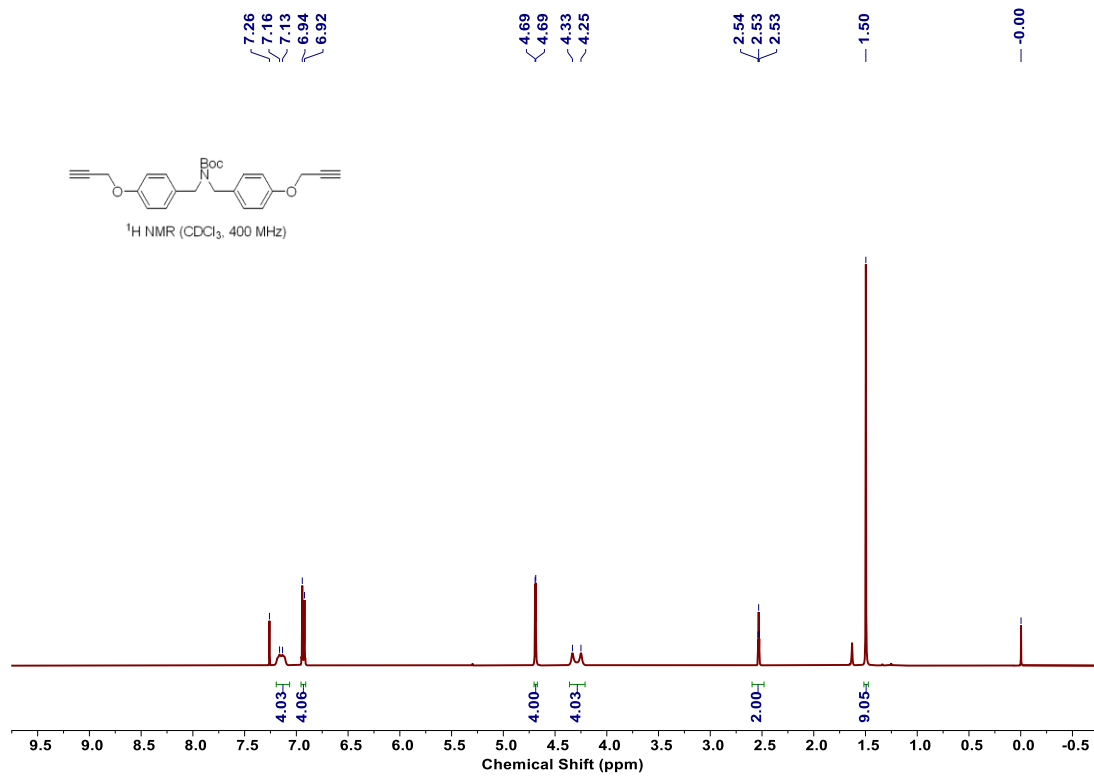
¹H NMR of compound 4a



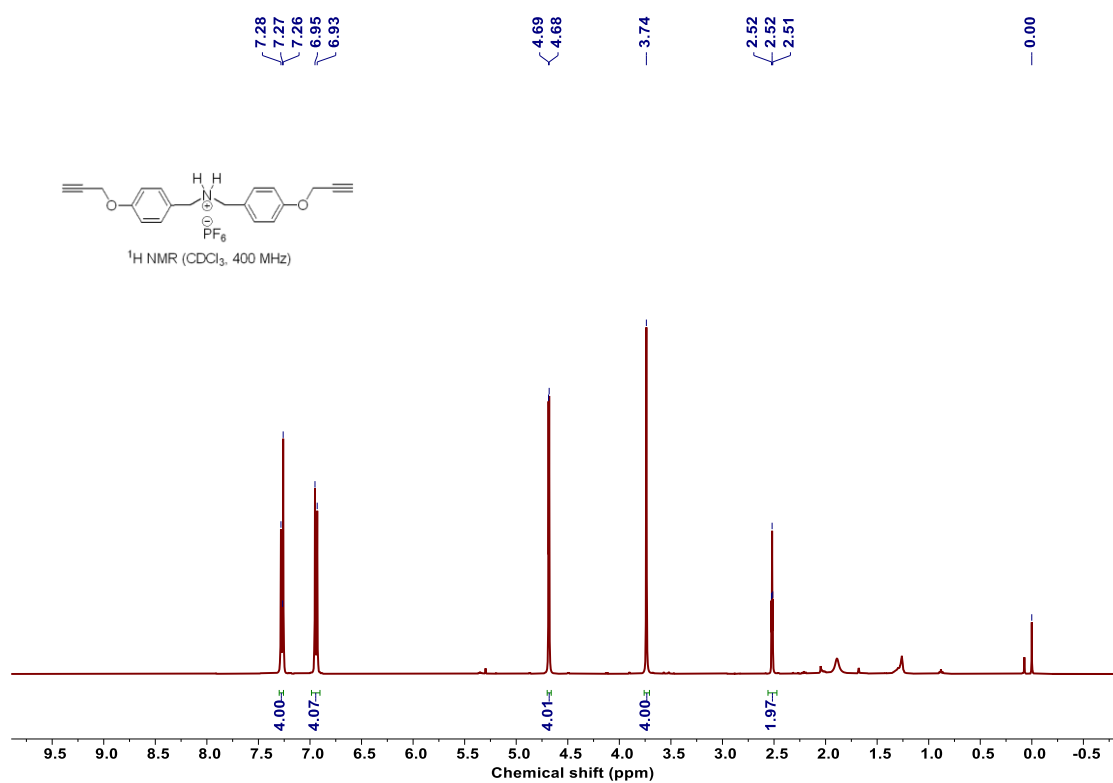
¹H NMR of compound **4b**



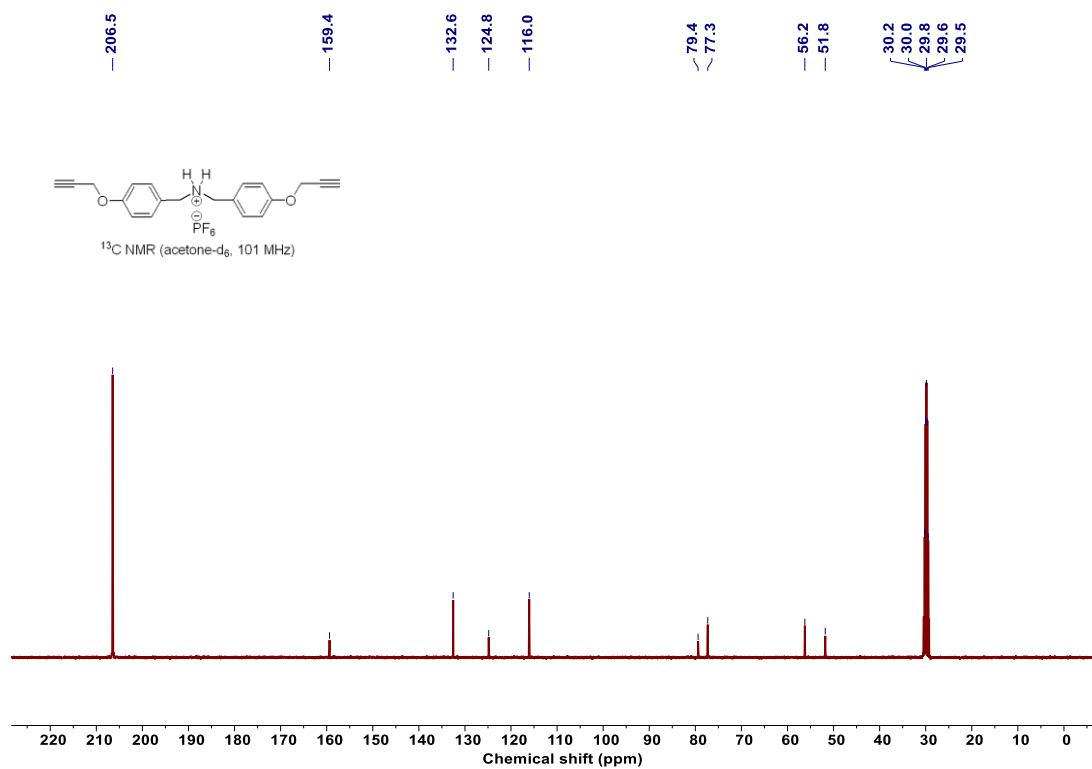
¹H NMR of compound **4c**



¹H NMR of compound 4

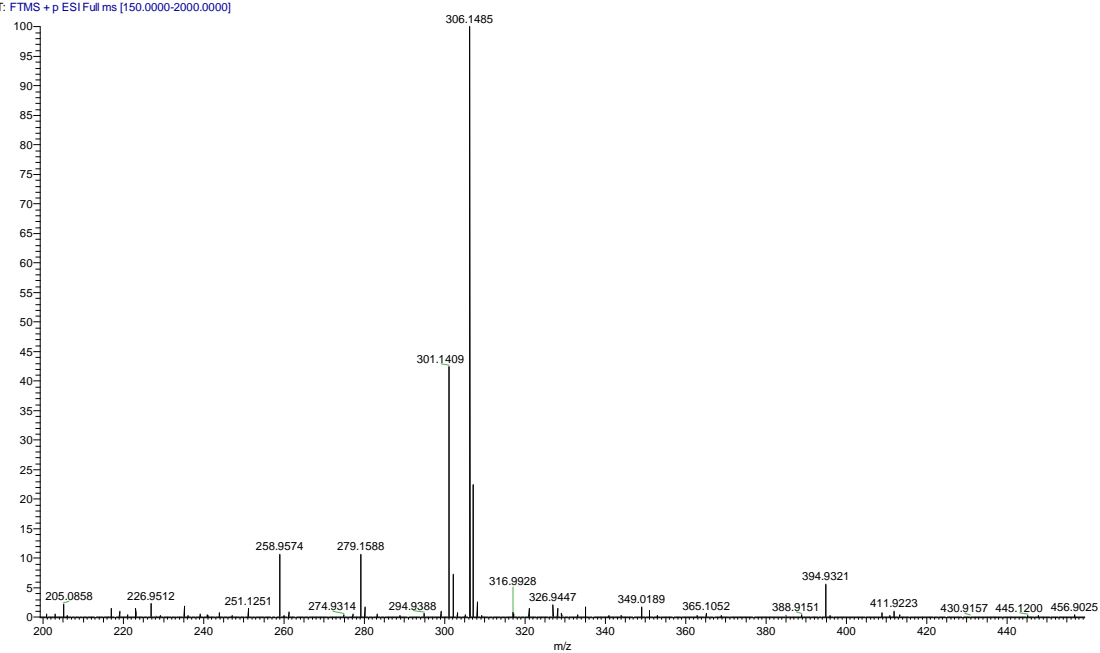


¹³C NMR of compound 4



HRMS of compound 4

2 #591 RT: 5.82 AV: 1 NL: 4.68E7
T: FTMS + p ESI Full ms [150.0000-2000.0000]



¹H NMR of compound 5

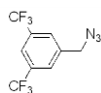
7.86

7.79

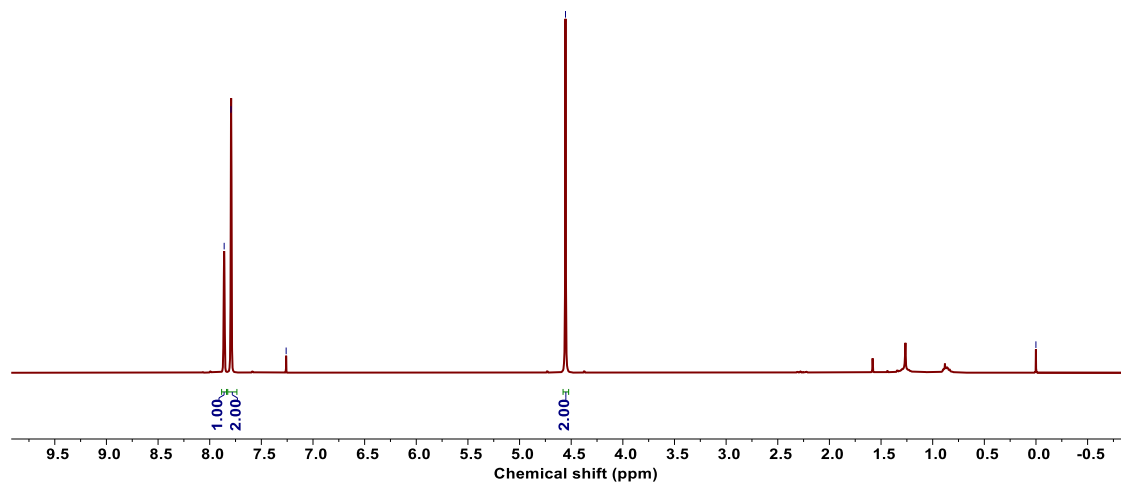
7.26

4.56

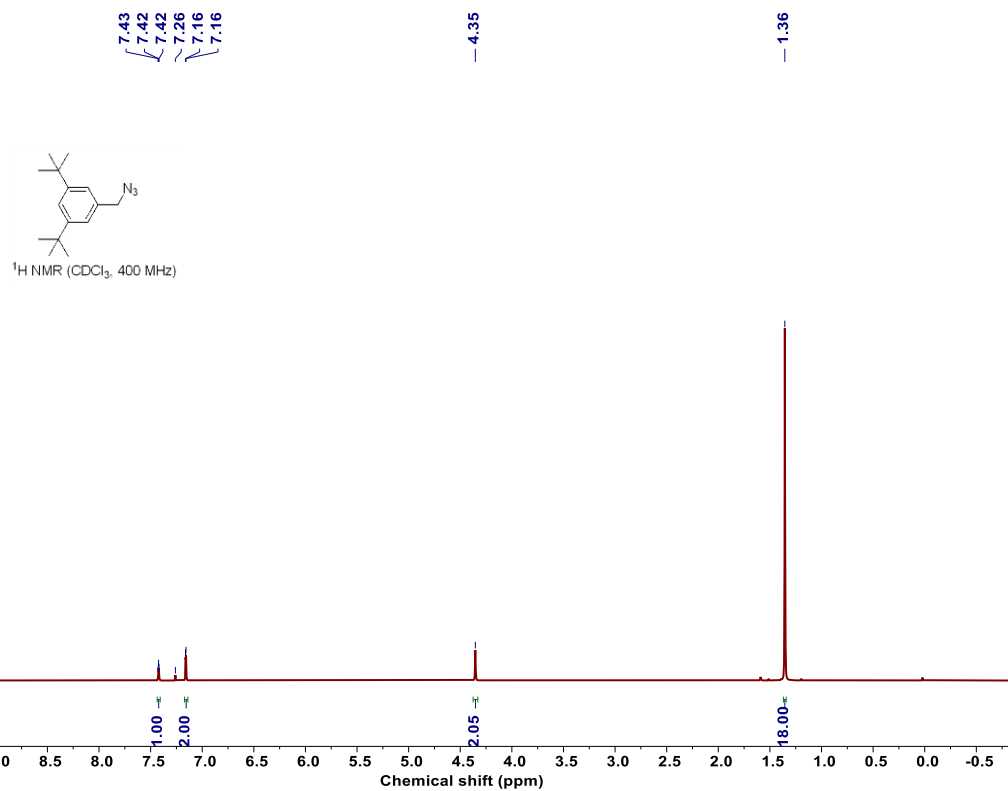
0.00



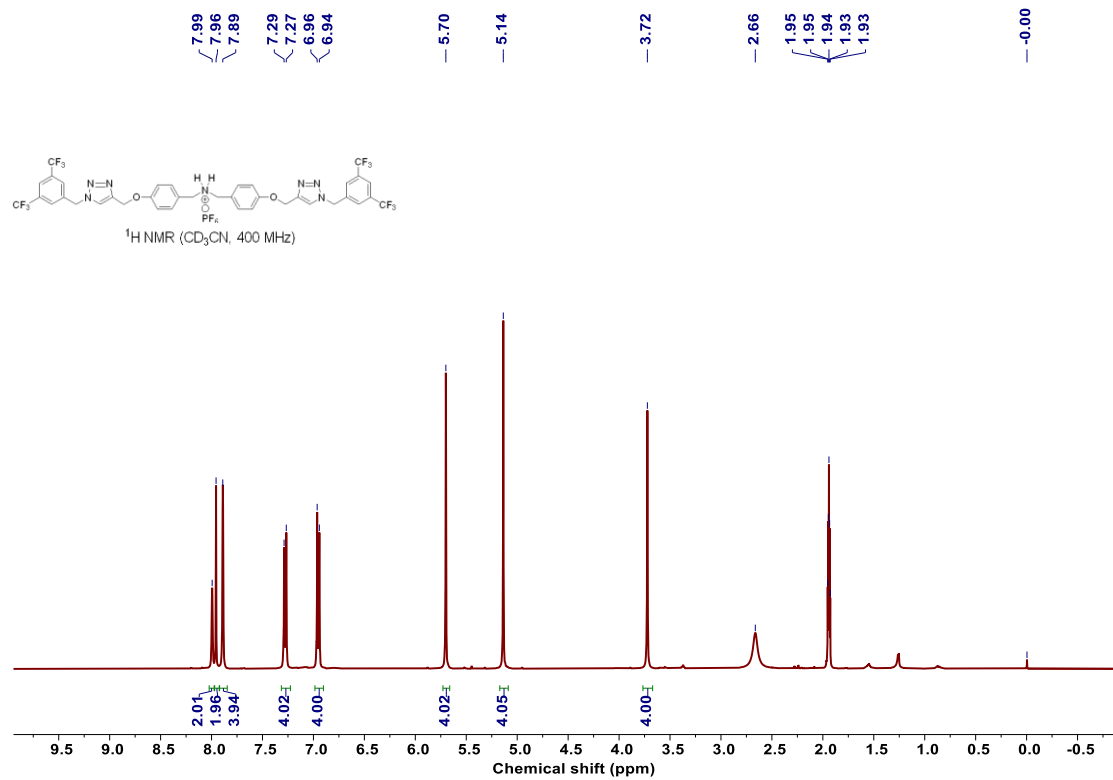
¹H NMR (CDCl₃, 400 MHz)



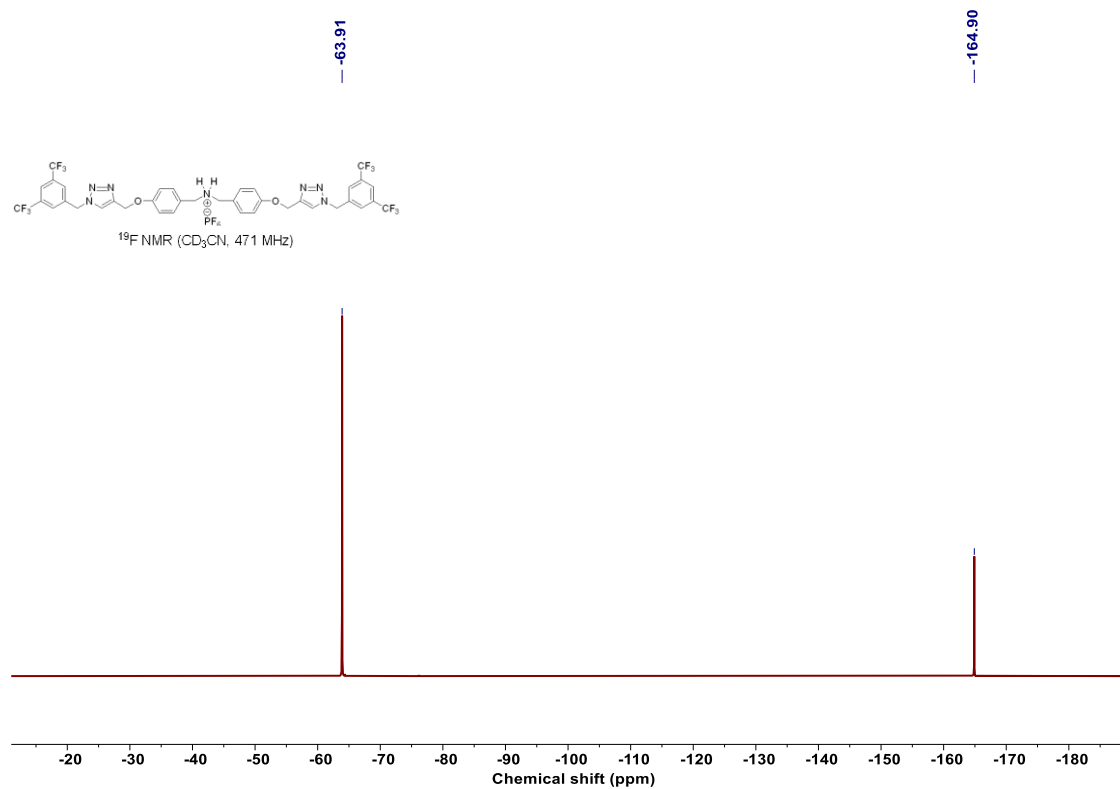
¹H NMR of compound **6**



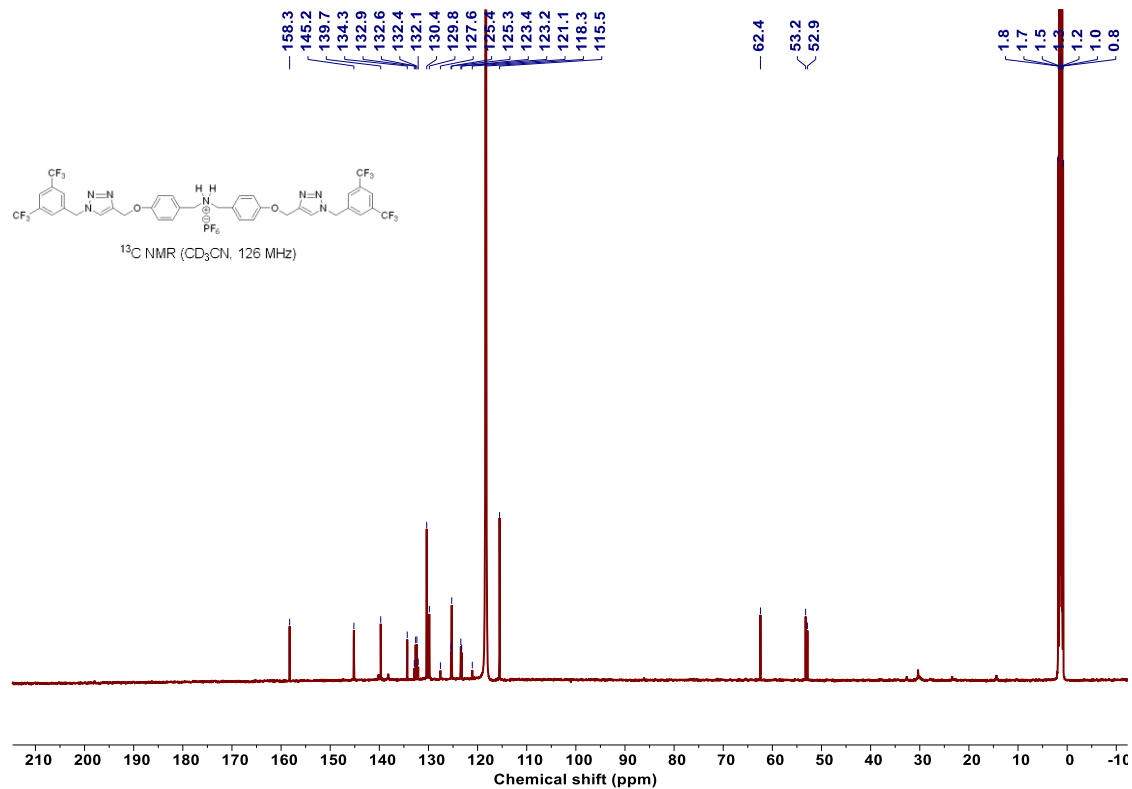
¹H NMR of axle **A₁**



¹⁹F NMR of axle A₁

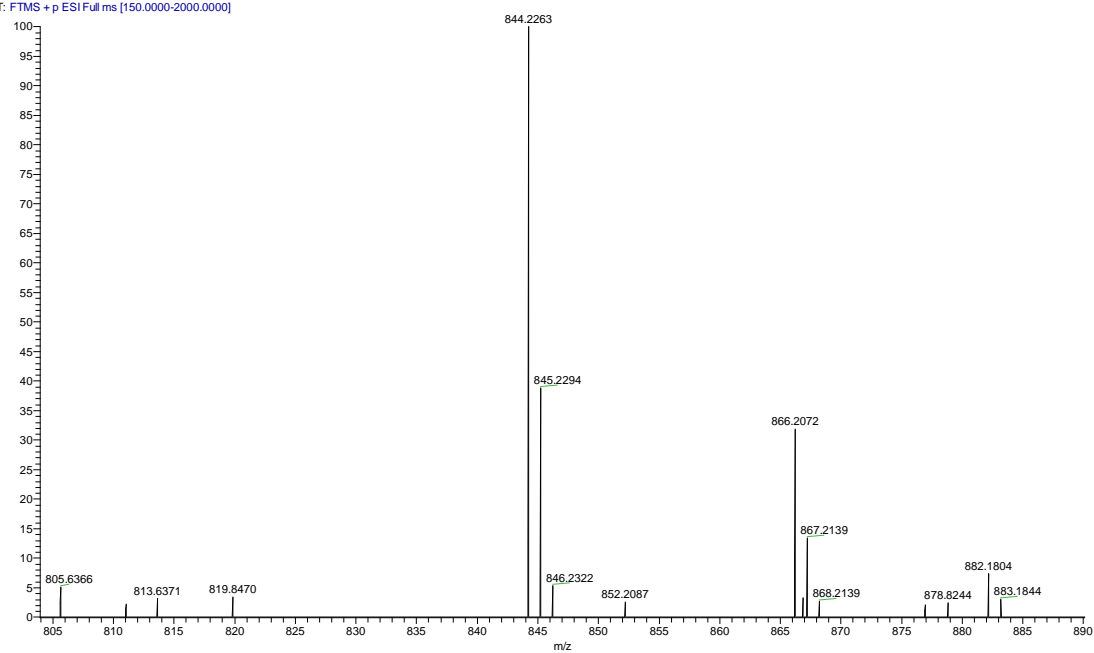


¹³C NMR of axle A₁



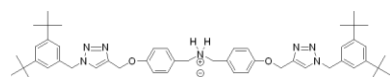
HRMS of axle A₁

3 #945 RT: 9.34 AV: 1 NL: 4.58E5
T: FTMS + p ESI Full ms [150.0000-2000.0000]

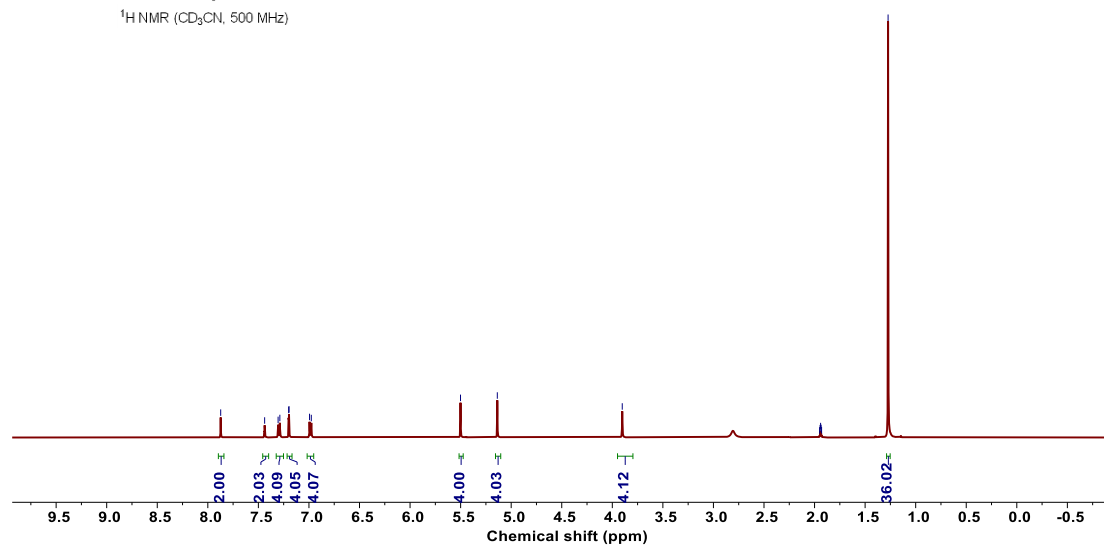


¹H NMR of axle A₂

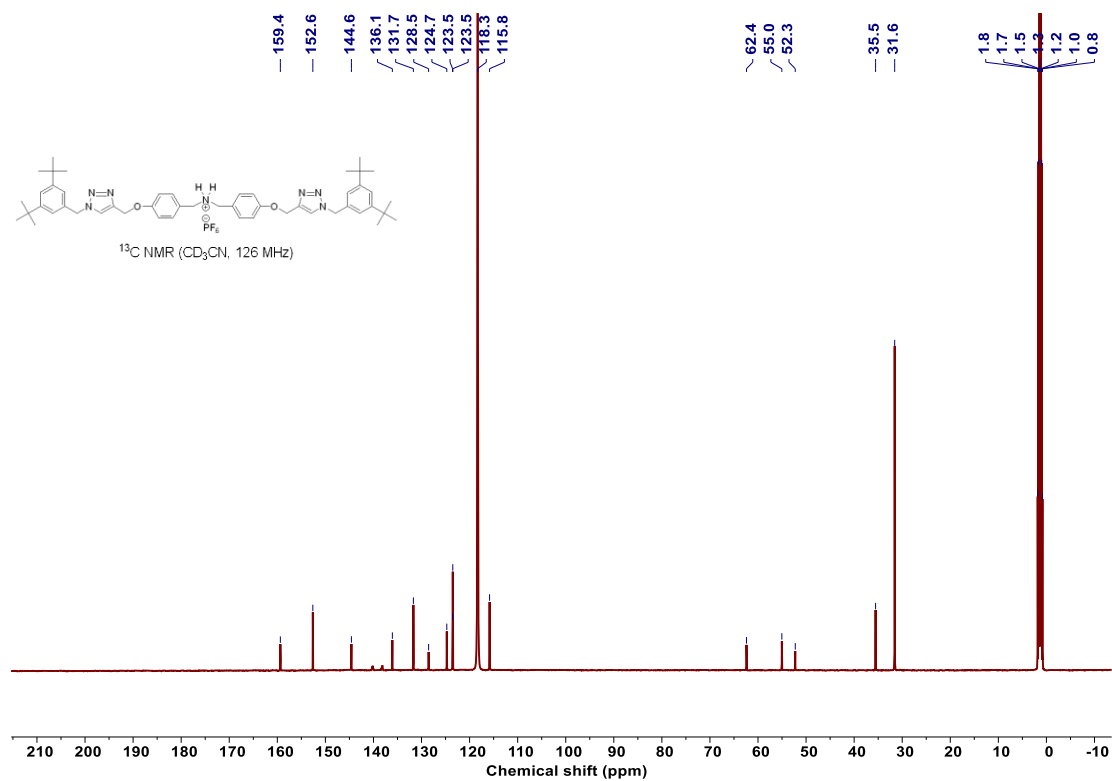
7.87, 7.44, 7.30, 7.29, 7.20, 7.20, 6.99, 6.98, 5.50, 5.14, 3.90, 1.95, 1.95, 1.94, 1.93, 1.27



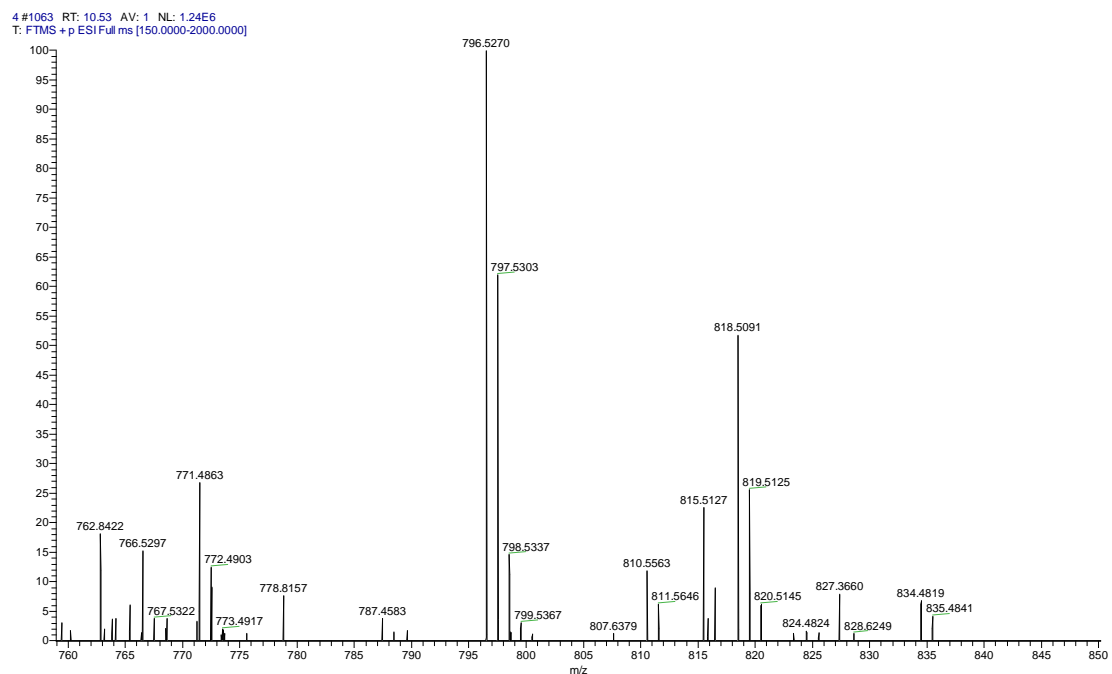
¹H NMR (CD₃CN, 500 MHz)



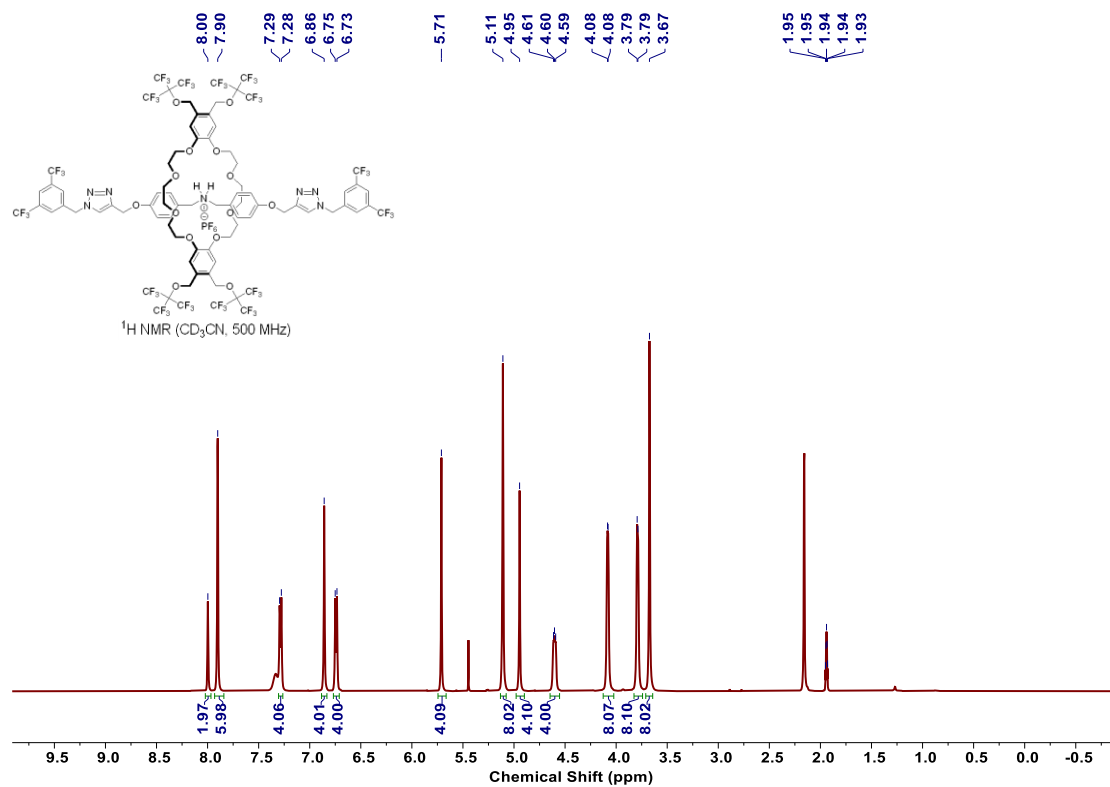
¹³C NMR of axle A₂



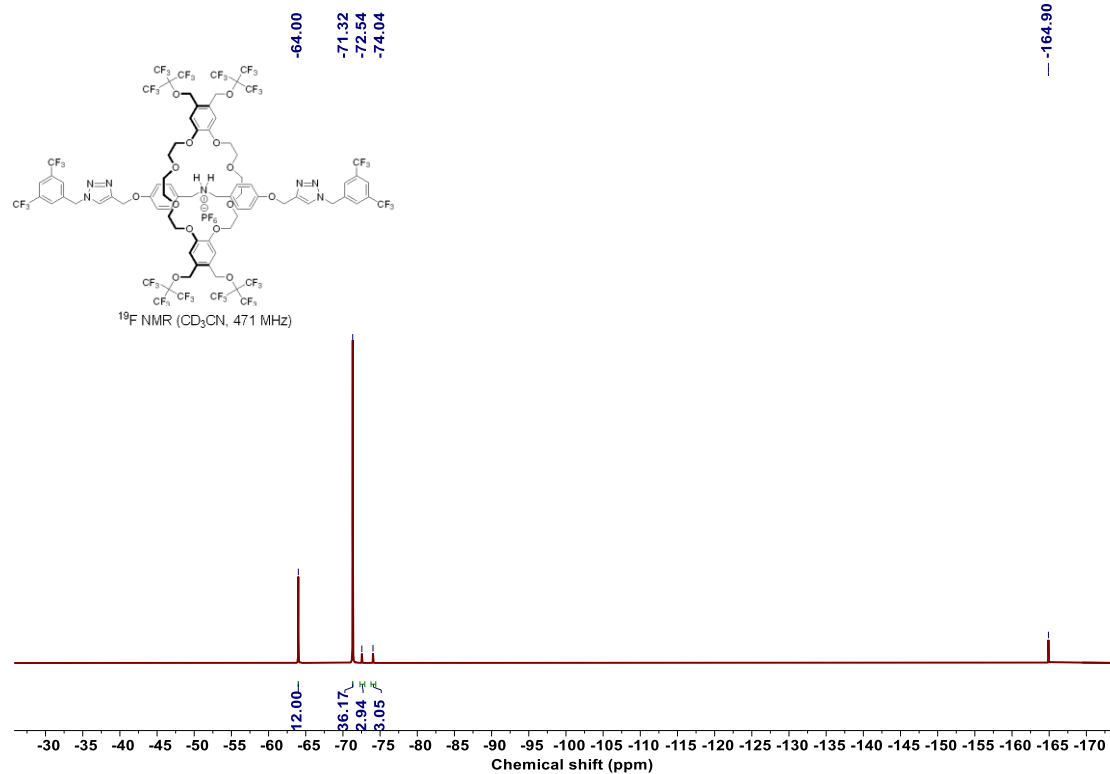
HRMS of axle A₂



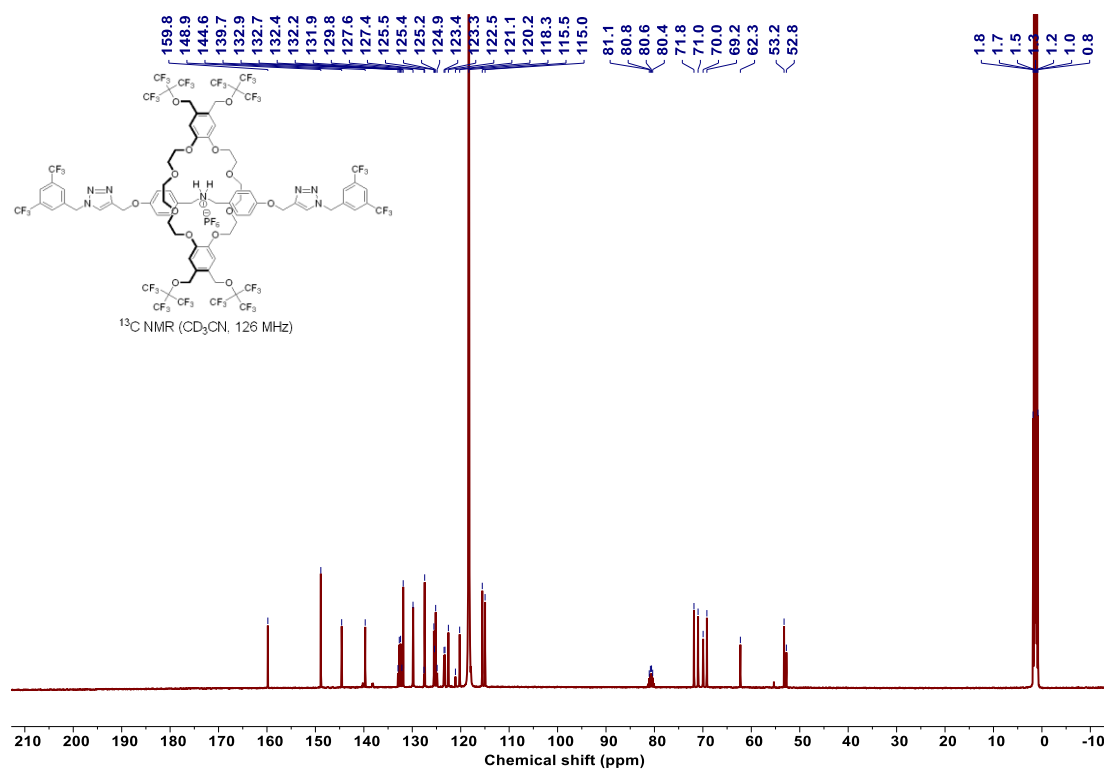
¹H NMR of [2]rotaxane **Rx-1**



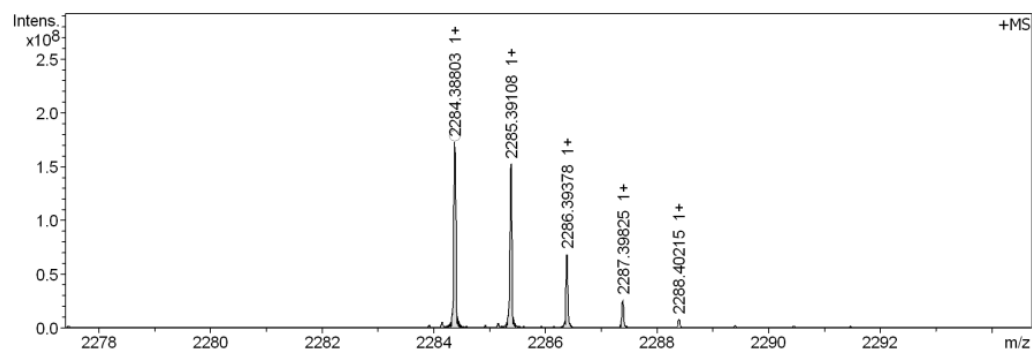
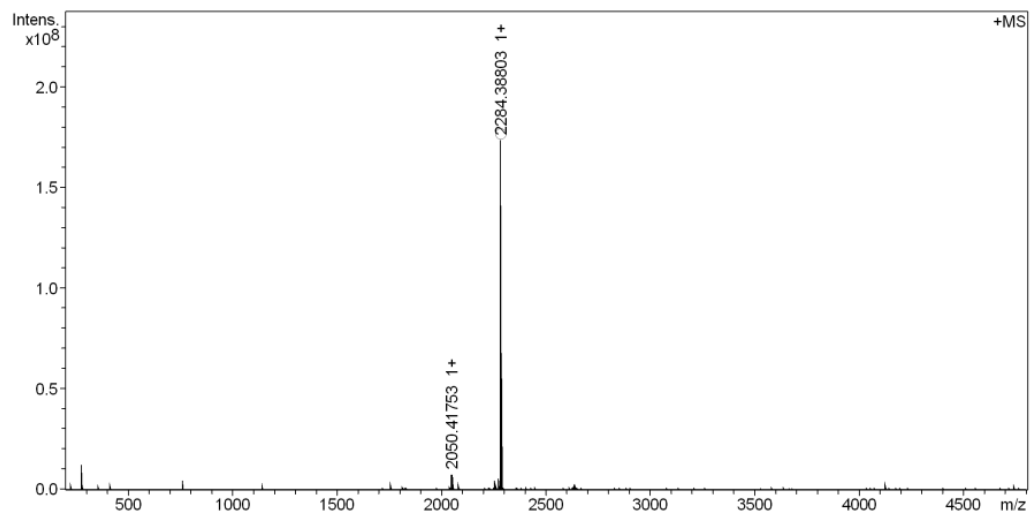
¹⁹F NMR of [2]rotaxane **Rx-1**



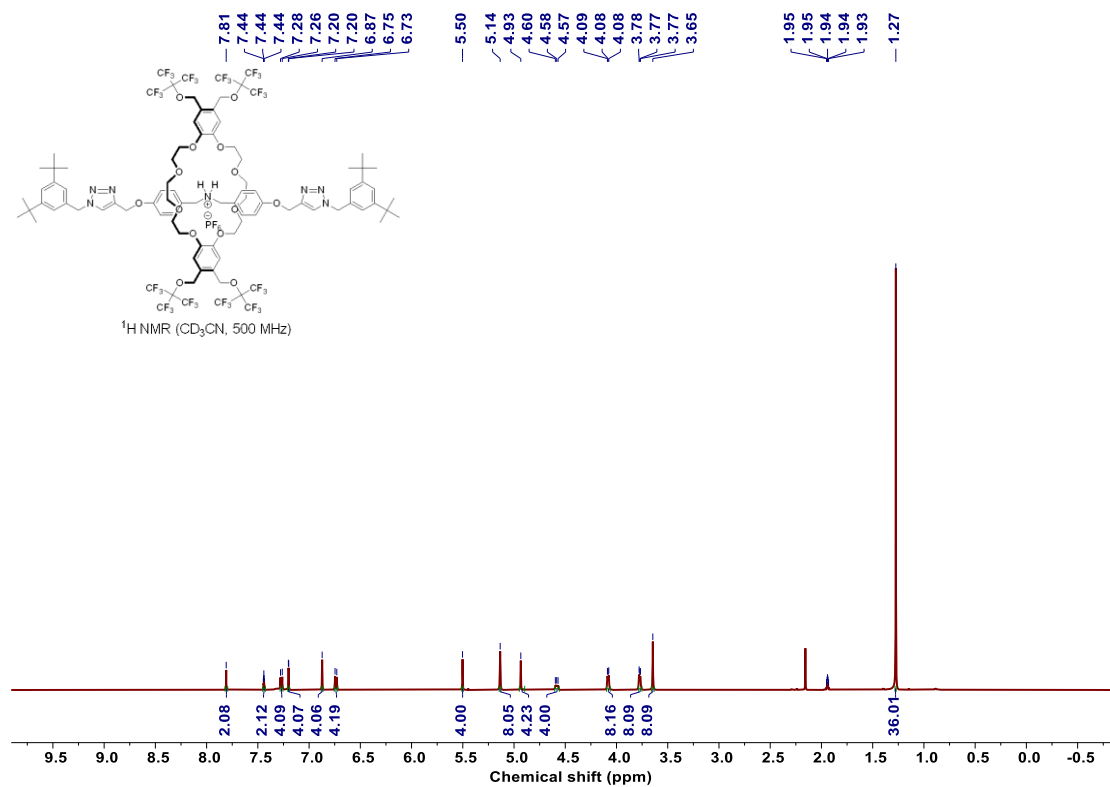
¹³C NMR of [2]rotaxane **Rx-1**



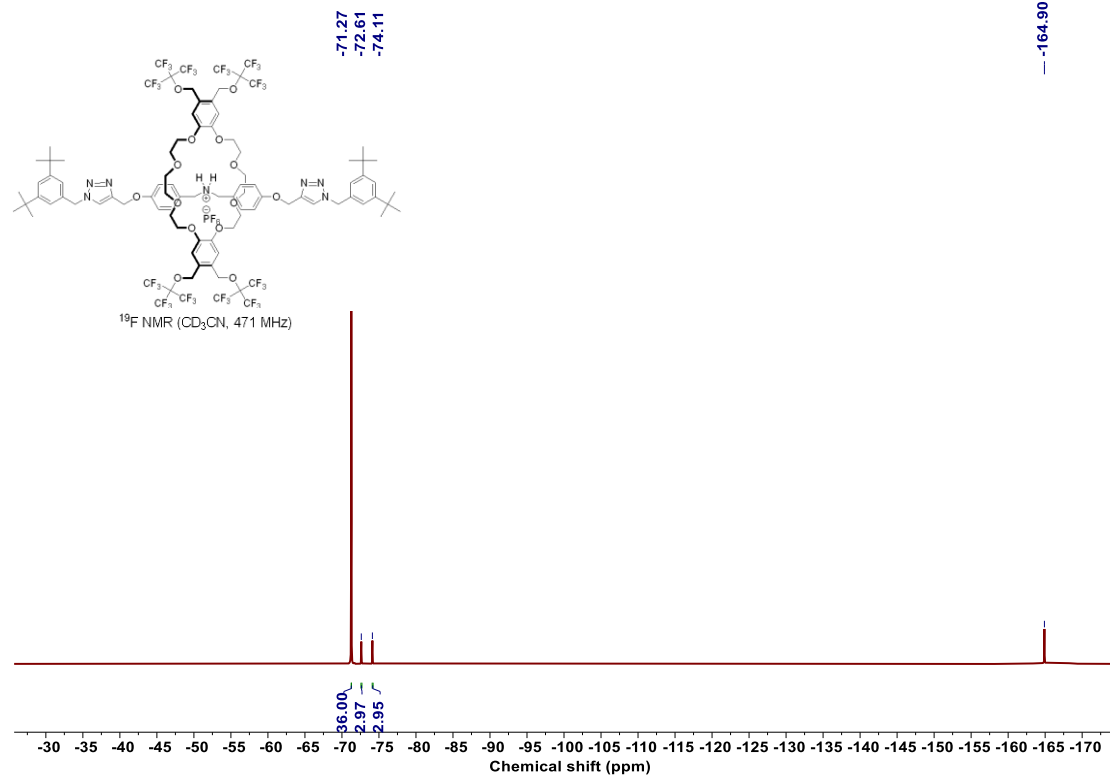
MALDI-FT-MS spectra of [2]rotaxane **Rx-1**



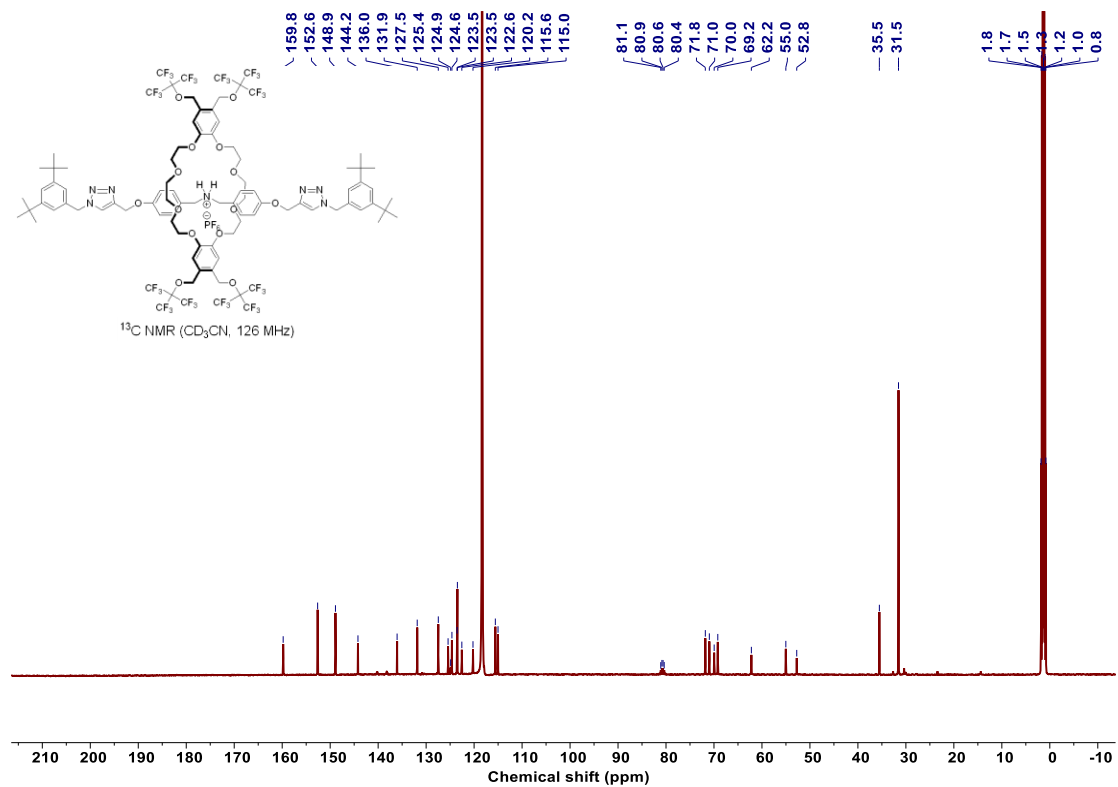
¹H NMR of [2]rotaxane **Rx-2**



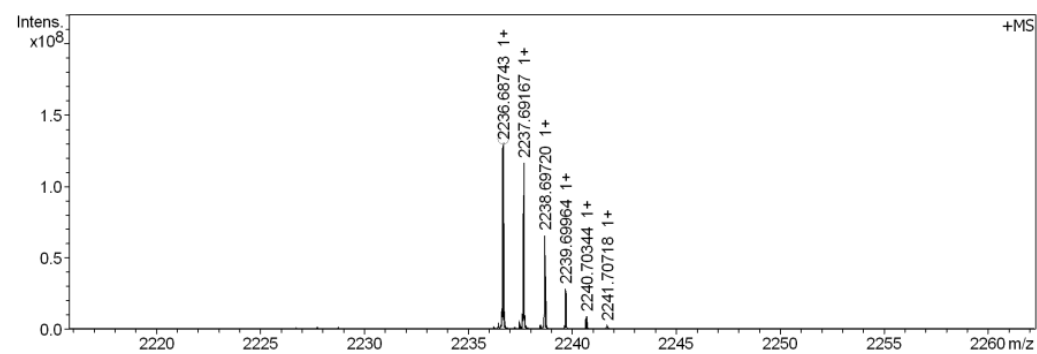
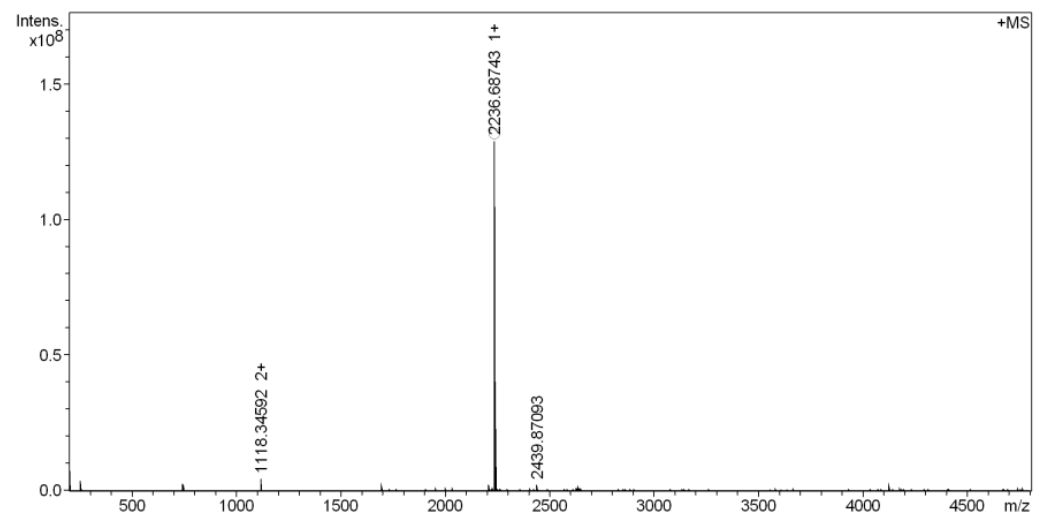
¹⁹F NMR of [2]rotaxane **Rx-2**



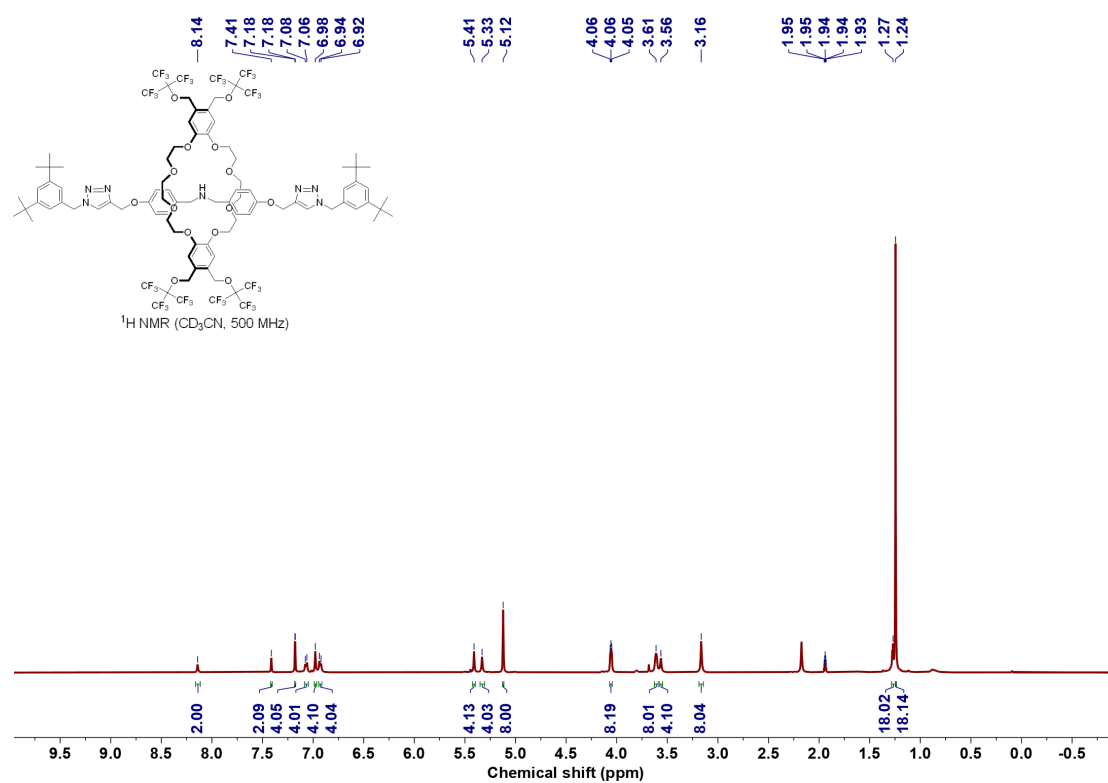
¹³C NMR of [2]rotaxane **Rx-2**



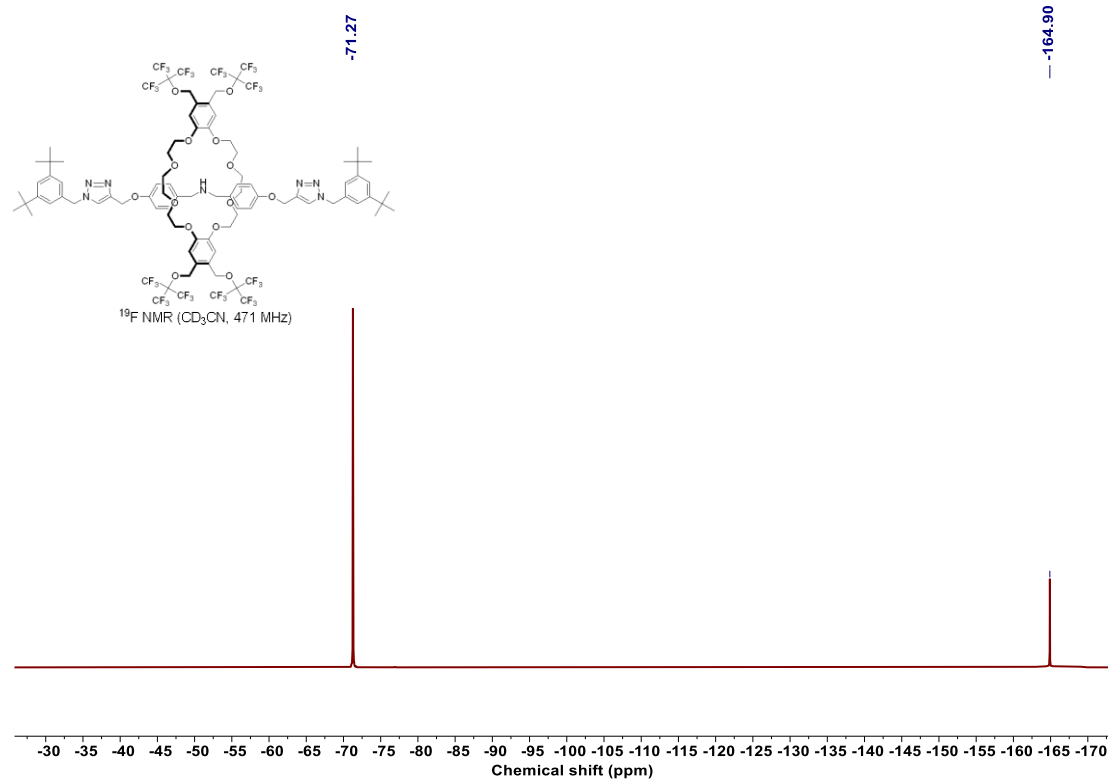
MALDI-FT-MS mass spectra of [2]rotaxane **Rx-2**



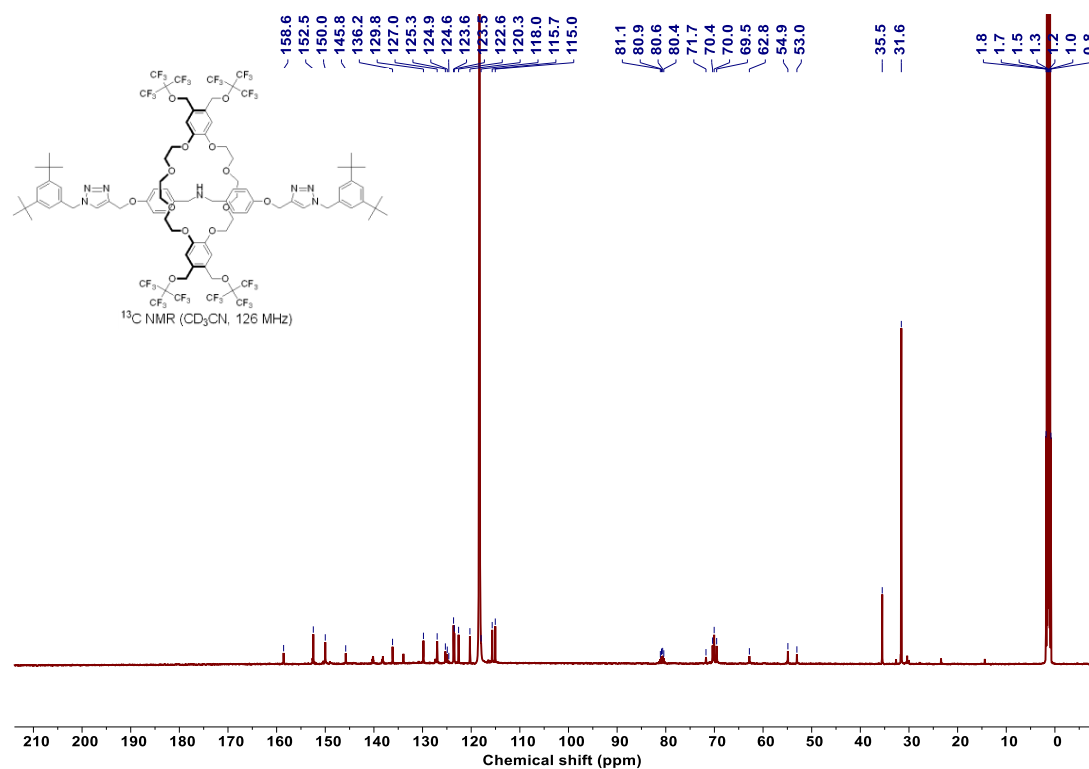
¹H NMR of [2]rotaxane **Rx-2'**



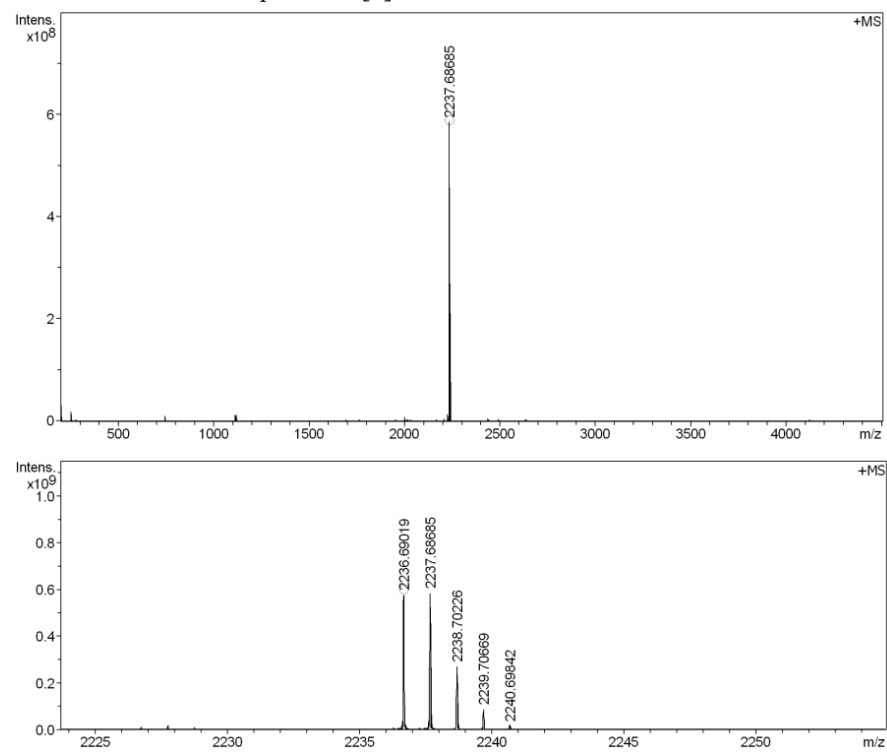
¹⁹F NMR of [2]rotaxane **Rx-2'**



¹³C NMR of [2]rotaxane **Rx-2'**



MALDI-FT-MS mass spectra of [2]rotaxane **Rx-2'**



References

- [1] D.J. Mercer, J. Yacoub, K. Zhu, S.K. Loeb, S.J. Loeb, *Org. Biomol. Chem.* 10 (2012) 6094-6104.
- [2] Z. Li, W. Liu, J. Wu, S. H. Liu, J. Yin, *J. Org. Chem.* 77 (2012) 7129-7135.
- [3] Y. Jiang, X.-Z. Zhu, C.-F. Chen, *Chem. - Eur. J.* 16 (2010) 14285-14289.
- [4] V. Blanco, A. Carlone, K.D. Hänni, D. A. Leigh, B. Lewandowski, *Angew. Chem. Int. Ed.* 51 (2012) 5166-5169.
- [5] C.-S. Kwan, R. Zhao, M.A. Van Hove, Z. Cai, K. C.-F. Leung, *Nat. Commun.* 9 (2018) 497.
- [6] W.G. Kim, M.E. Kang, J.B. Lee, et al., *J. Am. Chem. Soc.* 139 (2017) 12121-12124.
- [7] M. Curcio, F. Nicoli, E. Paltrinieri, et al., *J. Am. Chem. Soc.* 143 (2021) 8046-8055.
- [8] L. Martínez, R. Andrade, E.G. Birgin, J. M. Martinez, *J. Comput. Chem.* 30 (2009) 2157-2164.
- [9] R. Salomon-Ferrer, A.W. Götz, D. Poole, S. Le Grand, R. C. Walker, *J. Chem. Theory Comput.* 9 (2013) 3878-3888.
- [10] M. J. Frisch, G. H. Trucks, B. Schlegel, et al. *Gaussian 09 Revision A.1.* Gaussian Inc. 2009.
- [11] C.I. Bayly, P. Cieplak, W. Cornell, P. A. Kollman, *J. Phys. Chem.* 97 (1993) 10269-10280.
- [12] J. Wang, R.M. Wolf, J.W. Caldwell, P. A. Kollman, D. A. Case, *J. Comput. Chem.* 25 (2004) 1157-1174.
- [13] D.R. Roe, T.E. Cheatham III, *J. Chem. Theory Comput.* 9 (2013) 3084-3095.
- [14] V.N. Maiorov, G.M. Crippen, *J. Mol. Biol.* 235 (1994) 625-634.
- [15] C. Dalvit, M. Piotto. *Magn. Reson. Chem.* 55 (2017) 106-114.
- [16] M. Lu, R. Ishima, T. Polenova, A.M. Gronenborn. *J. Biomol. NMR* 73 (2019) 401-409.
- [17] X. Lu, C. Huang, M. Li, et al., *Phys. Chem. B* 124 (2020) 5271-5283.